# REPORT DOCUMENTATION PAGE

Form Approved
OMB No. 0704-0188

Public reporting burden for this collection of information is estimated to average 1 hour per response, including the time for reviewing instructions, searching existing data sources, gathering and maintaining the data needed, and completing and reviewing the collection of information. Send comments regarding this burden estimate or any other aspect of this collection of information, including suggestions for reducing this burden, to Washington Headquarters Services, Directorate for Information Operations and Reports, 1215 Jefferson Davis Highway, Suite 1204, Arlington, VA 22202-4302, and to the Office of Management and Budget, Paperwork Reduction Project (0704-0188), Washington, DC 20503.

| 1. AGENCY USE ONLY (Leave blank) | 2. REPORT DATE<br>October 10, 1997 | 3. REPORT TYPE AND DATES COVERED<br>Final Report 1-6-93 To 31-5-97 | |
|---|---|---|---|
| 4. TITLE AND SUBTITLE<br>New Approaches to Aluminum Passivation for Corrosion Prevention | | | 5. FUNDING NUMBERS<br>F49620-93-1-0341<br>3484/XS<br>61103D |
| 6. AUTHOR(S)<br>John T. Yates, Jr. | | | |
| 7. PERFORMING ORGANIZATION NAME(S) AND ADDRESS(ES)<br>University of Pittsburgh<br>Pittsburgh, PA 15260 | | | 8. PERFORMING ORGANIZATION REPORT NUMBER<br>AFOSR-TR-97<br>0560 |
| 9. SPONSORING/MONITORING AGENCY NAME(S) AND ADDRESS(ES)<br>Capt. Hugh C. DeLong<br>Air Force Office of Scientific Research<br>Directorate of Chemistry and Life Sciences<br>110 Duncan Avenue Suite B115<br>Bolling Air Force Base, DC 20332-8080 | | | 10. SPONSORING/MONITORING AGENCY REPORT NUMBER |
| 11. SUPPLEMENTARY NOTES | | | |

| 12a. DISTRIBUTION/AVAILABILITY STATEMENT<br>Approved for public release;<br>distribution unlimited. | 12b. DISTRIBUTION CODE |
|---|---|

**13. ABSTRACT (Maximum 200 words)**

**19971103 080**

A new method has been discovered for producing a corrosion-resistant aluminum oxide film on aluminum surfaces. The method employs the electronic activation of adsorbed water molecules on the aluminum surface, using electron-bombardment. The artificial oxide film, so produced, exhibits about 25 times higher electrical impedance using electrochemical measurements compared to aluminum oxide films made by conventional oxidation.

| 14. SUBJECT TERMS<br>Aluminum, aluminum oxides, corrosion, passivation, electron impact | | | 15. NUMBER OF PAGES<br>4 |
|---|---|---|---|
| | | | 16. PRICE CODE |
| 17. SECURITY CLASSIFICATION OF REPORT<br>U | 18. SECURITY CLASSIFICATION OF THIS PAGE<br>U | 19. SECURITY CLASSIFICATION OF ABSTRACT<br>U | 20. LIMITATION OF ABSTRACT<br>UL |

NSN 7540-01-280-5500

Standard Form 298 (Rev. 2-89)
Prescribed by ANSI Std. Z39-18

DTIC QUALITY INSPECTED 3

# FINAL REPORT

## New Approaches to Aluminum Passivation for Corrosion Prevention

John T. Yates, Jr.
Department of Chemistry
Surface Science Center
University of Pittsburgh
Pittsburgh, PA 15260
(412)-624-8320

## I. Objective

The objective of this research was to discover new methods for producing a corrosion passivation layer on aluminum surfaces, and for measuring the degree of corrosion passivation using electrochemical methods. This objective has been achieved. The work was divided into two parts. In the first part, an Al(111) single crystal surface was employed to study the activation of adsorbed water molecules with low energy electrons, leading to an artificial oxide layer. In the second part, the method developed in the work with the Al(111) crystal was applied to many polycrystalline Al samples and the artificial oxide films produced were then tested by electrochemical impedance spectroscopy for their ability to retard electrochemical corrosion.

## II. Status of Effort

The two objectives described above have been completely achieved. To do this, the production of artificial aluminum oxide films was carefully studied using X-ray photoelectron spectroscopy and electron energy loss spectroscopy. The efficiency of the production of the artificial oxide film was measured and found to be very high for 100 eV electrons. Subsequent studies on polycrystalline samples of aluminum were also carried out, and it was shown in comparisons between 18 different experiments that artificial oxide films were about 25 times more resistant

to electrochemical corrosion compared to control experiments on oxide films produced by conventional methods involving exposure to water vapor and to air.

## III. Accomplishments/New Findings

1. Water is efficiently converted to $Al_2O_3$ on $Al(111)$ by electrons with a cross section of about $2 \times 10^{-16}$ $cm^2$ for 100 eV electrons.

2. The $Al_2O_3$ layer displays a bulk plasmon mode near 23.7 eV, in agreement with that observed for aluminum oxide produced by conventional methods.

3. The threshold electron energy for the excitation is near 6 eV and corresponds to a dissociative electron attachment process in water.

4. The ratio of Al/O in the artificial film is 2/3.

5. The Al(2p) and O(1s) binding energies in the artificial oxide film are in accordance that in bulk $Al_2O_3$.

6. The artificial aluminum oxide film displays a bandgap of 5.5 eV, which is the same as seen for sapphire using the electron energy loss technique.

7. The film grows during electron bombardment to a limiting thickness of 25 A by means of linear kinetics.

8. The electrochemical impedance spectroscopy measurements indicate that the oxide film grown artificially is about 25 times higher in average impedance than equivalent thickness films grown by conventional oxidation methods.

The results leading to the first 7 conclusions are shown in the progress report written on the primary AFOSR project (September 18, 1997). The results leading to the important conclusion, number 8, are shown in the Figure attached. These results are important because they show that at low frequencies, where the film impedance is measured independent of other impedances in the circuit, a large

2

large difference in average film impedance is reproducibly found. The measurements indicate that the average factor increase in impedance is of the order of 25, with factor differences ranging up to 100 or more being observed. This difference is probably due to porosity differences in the films, with the artificial film being much less porous than the air oxidized film.

## IV. Personnel

Graduate Student: Mr. Thomas Barefoot

## V. Publications

1. T. P. Barefoot, H. D. Ebinger, and J. T. Yates, Jr., "Low Energy Broad Beam Electron Gun," J. Vac. Sci. Technol., A15, 2740 (1997). *

This paper was critical to being able to achieve the results leading to the conclusions 1-8 listed above. A copy of the paper is included with this report.
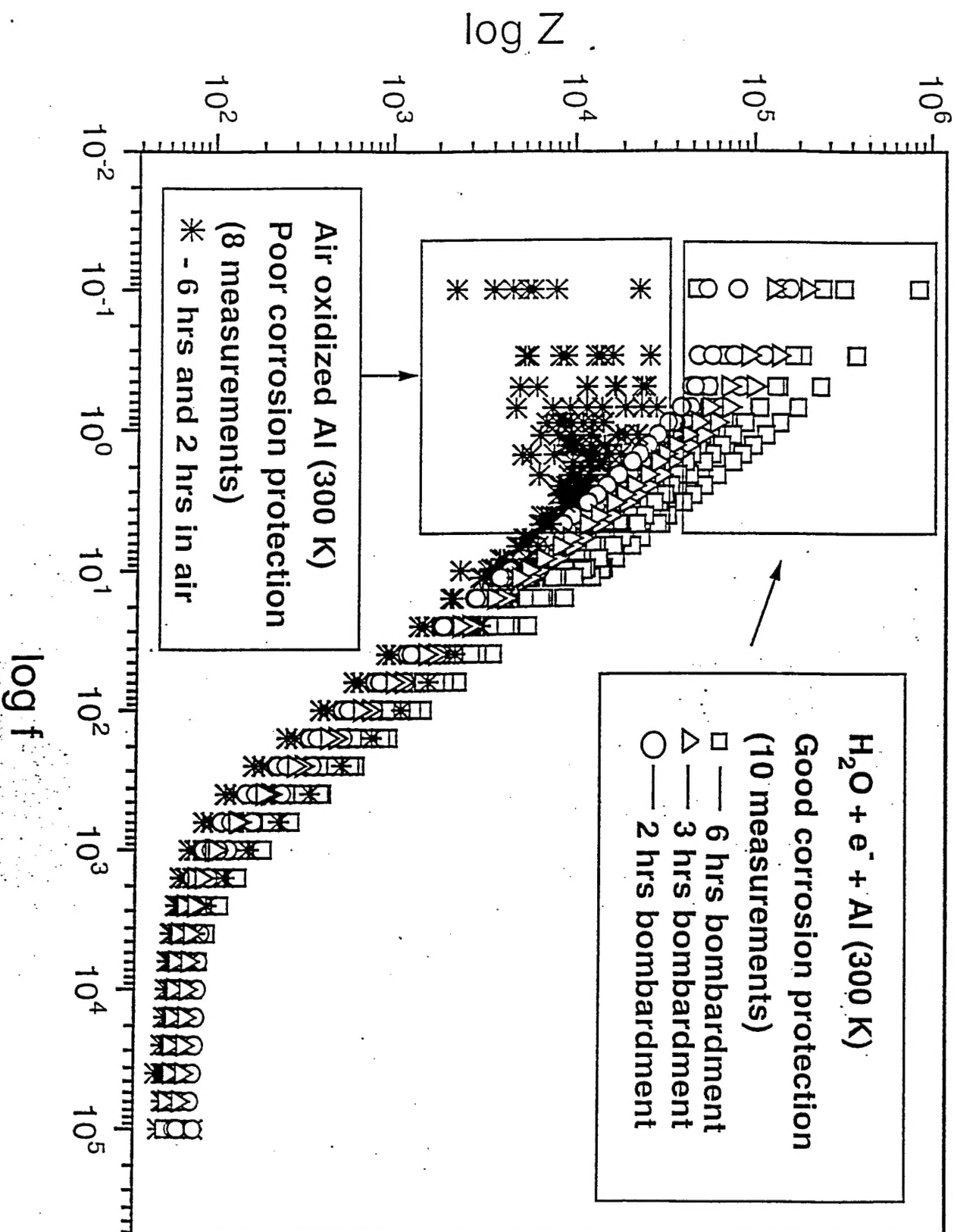
*A number of other publications were produced in the area of this project but do not include the AASERT student as co-author. The additional publications include the following:

## IV. Publications:

1. H. D. Ebinger and J. T. Yates, Jr., "Oxidation of Al(111) by Electron Impact on Adsorbed $H_2O$," accepted, Surface Science.

2. H. D. Ebinger and J. T. Yates, Jr., "Electron Impact Induced Oxidation of Al(111) in Water Vapor - Relation to the Cabrera-Mott Mechanism," accepted, Phys. Rev. B.

3.  A. Kuznetsova, E. A. Wovchko and J. T. Yates, Jr.,
    "FTIR Study of the Adsorption and Thermal Behavior of
    Vinyltriethoxysilane Chemisorbed on $\gamma$-Al$_2$O$_3$," accepted, Langmuir.

4.  I. Popova and J. T. Yates, Jr., "Adsorption and Thermal
    Behavior of Benzotriazole Chemisorbed on $\gamma$-Al$_2$O$_3$,"
    accepted, Langmuir.

# H₂O + e⁻ and Air Oxidized Aluminum



**log Z** (vertical axis): $10^2$, $10^3$, $10^4$, $10^5$, $10^6$

**log f** (horizontal axis): $10^{-2}$, $10^{-1}$, $10^0$, $10^1$, $10^2$, $10^3$, $10^4$, $10^5$

Air oxidized Al (300 K)
Poor corrosion protection
(8 measurements)
✳ – 6 hrs and 2 hrs in air

H₂O + e⁻ + Al (300 K)
Good corrosion protection
(10 measurements)
□ — 6 hrs bombardment
△ — 3 hrs bombardment
○ — 2 hrs bombardment

# Low-energy broad beam electron gun

Thomas W. Barefoot, Hans D. Ebinger, and John T. Yates, Jr.[a]
*Surface Science Center, Department of Chemistry, University of Pittsburgh, Pittsburgh, Pennsylvania 15260*

A low-energy electron gun for the energy range of 5–100 eV providing a uniform and high electron flux over a circular surface area of several $cm^2$ has been designed and tested. Focusing elements allow one to vary the beam diameter according to experimental needs. The uniform current densities make it suitable for the study of electron stimulated surface chemistry and thin-film production. © *1997 American Vacuum Society.* [S0734-2101(97)06205-2]

## I. INTRODUCTION

Electron sources are of great importance for the study of surface chemistry. Many surface sensitive analytical techniques employ electron excitation of the sample,[1] since the electron mean-free path in solids for convenient laboratory acceleration voltages is of the order of only a few Angstroms.[2] Furthermore, the de Broglie wavelength of electrons with energies of a few hundred electron volts allows surface diffraction. Low-energy electrons with kinetic energies of 5–10 electron volts are used for vibrational spectroscopy.[3] For charge neutralization of insulator surfaces, electron emitters are sometimes operated without any acceleration voltage.[4] Electron guns for these various methods have to meet special constraints on electron energy, beam current, energy width, beam diameter, resolution, coherence, etc. In general, every analytical method dealing with electron bombardment of the sample has its specific needs and, therefore, special electron gun designs have been developed.[5]

It is well known that the probing electron beam often alters the surface under investigation. The observed effects extend from simple charging of insulating samples to chemical modifications of the sample surface. Electronic excitations of adsorbed molecules cause ionization, dissociation, desorption, and nonthermal chemical reactions.[6] Based on these observations, a whole field of electron induced surface chemistry has been developed, allowing refined techniques in surface modification, like writing oxide structures on semiconductor and metal surfaces.[7]

In order to investigate electron stimulated chemistry with all of the analytical techniques available in an ultrahigh vacuum system, the uniform irradiation of the entire sample is often needed. This makes feasible analytical methods, which average over a wide surface area. Broad beam electron sources are, therefore, required. The relevant electronic excitation energies for dissociation or desorption, typically, are of the order of 10 eV, which means that the energy resolution should be considered in gun design, in order to be able to accurately determine energetic thresholds. In this article, we present an electron gun design, considering these constraints. The electron gun design provides an alternative to a design that has been published previously.[8] The gun design emphasizes energy resolution, beam focusing capability, and allows the sample to be at ground potential rather than being used at variable potential for beam focusing and acceleration.

## II. ELECTRON GUN DESIGN

### A. Potential settings and trajectory calculations

Design, potential setup, and trajectory calculations have been carried out using the three-dimensional (3D) ion optics program SIMION,[9] version 6.0. Figure 1 shows the elements of the low-energy electron gun. The design possesses cylindrical symmetry around the center cathode–sample axis. The true relative dimensions are shown. The source of electrons is a cathode disk emitter on axis. The potential of the cathode defines the beam energy if the sample is at ground potential (standard operation condition). Electron extraction from the near cathode region is done by an anode at positive potential in front of the emitter and a repeller at a more negative potential than the cathode. The gun works with high electric fields near the cathode in order to achieve efficient extraction down to low electron energies. Therefore, the anode is at high positive potential relative to the emitter disk, resulting in a high kinetic energy of the electrons in this region. The beam then ''expands'' into the lens section (electrodes $E_1$–$E_4$). Four focusing elements, increasing in length, moving away from the emitter, have been employed. In the broad beam operation used for homogenous sample irradiation, they help to expand the beam. Their positive potential decreases, moving away from the anode, with the final electrode at ground potential. Alternatively, these elements can be employed for focusing. Figure 2 shows the electrostatic potential in the cathode region in a three-dimensional plot for electrons. The geometry and potential of the repeller and anode create a steep potential drop guiding the electrons into the electrode region. The shape of the potential is designed to increase the lateral momentum of the electrons in order to achieve a broad electron beam.

Figure 3 shows the calculated trajectories for electron energies of 100, 50, and 10 eV and a sample–gun distance of 25 mm from the end of the gun. The initial momentum of the emitted electrons has been set to be parallel to the center axis of the gun perpendicular to the cathode plane. The initial kinetic energy is 0.2 eV. The emission from the whole disk is taken into account. The potential setting for the electrodes

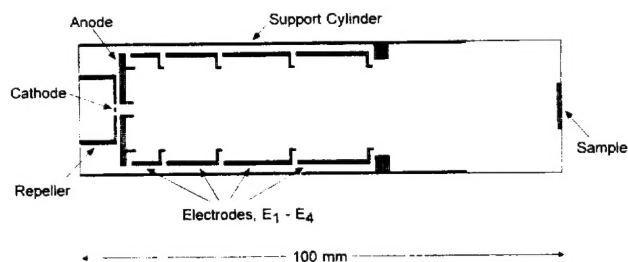[a]Electronic mail: JYATES@VMS.CIS.PITT.EDU

FIG. 1. Potential array used for trajectory calculations with the 3D ion optics program SIMION. The setup has cylindrical symmetry around the center axis from cathode to sample.

$(+30, +15, +5,$ and $0$ V going from $E_1$ to $E_4$) is the same in all three cases. Repeller and anode potential have been varied in order to achieve a uniform and fairly constant beam profile over this energy regime. As can be seen from the smoothly spaced electron trajectories, the sample is homogenously irradiated. Figure 4 shows how these two potentials vary with beam energy, when optimizing them in order to give a constant beam profile.

## B. Construction

Figure 5 shows the electron gun construction. The electron gun is supported on a $2\frac{3}{4}$ in. diam flange with a ten-pin electrical feedthrough. Two pins lead to the cathode and one to each of the repeller, anode, and the four electrodes. All elements are stacked inside a metal support cylinder, separated, and isolated by ceramic spacer rings. This makes assembly very easy and gives the required accuracy for element alignment. On both ends of the support cylinder there are terminal rings, which hold the elements in place. The lower one close to the cathode contains adjustment screws to align the center axis of the gun. The supporting cylinder is attached to the flange by a metal spacer, which has a number of cuts to allow access to the leads for assembly. The total length of our model is 140 mm measured from the flange to the end of the cylindrical support.
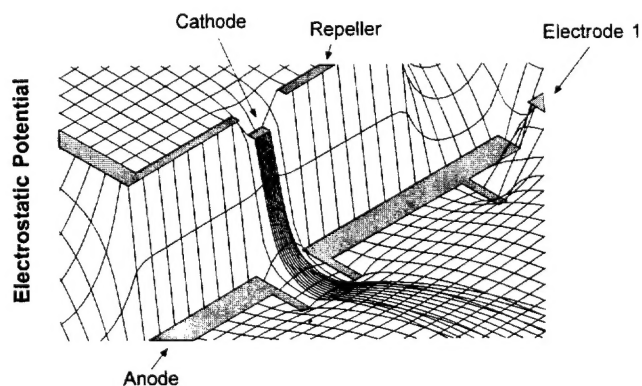


FIG. 2. The electrostatic potential for electrons in the cathode region. The high electric field produces effective extraction of electrons from the emitter. The geometry of the anode yields a potential shape, which increases the lateral momentum of the electrons in order to achieve a broad beam.
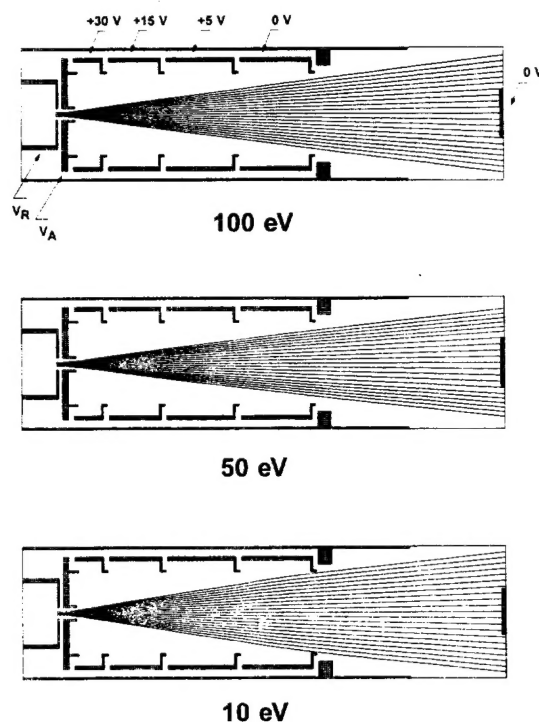


100 eV

50 eV

10 eV

FIG. 3. Electron trajectories for three different electron energies/cathode potentials. The electrode potentials are the same in all three cases $(+30, 15, 5,$ and $0$ V from $E_1$ to $E_4$). The repeller and anode potentials have been adjusted in order to achieve a constant beam profile. The anode potentials are $+200, +170,$ and $+100$ V, and the repeller potentials $-170, -105,$ and $-35$ V going from 100 to 50 to 10 eV beam energy.

The cathode disk and the ceramic rings are parts from commercial electron guns. The cathode is a BaO disk emitter[10] for which the mounting has been designed. It gives a high emission current at low, cathode temperatures, keeping pressure changes during operation low, and avoiding the production of undesirable species from a hot filament.[11] Optionally, a tantalum disk emitter is available on the same
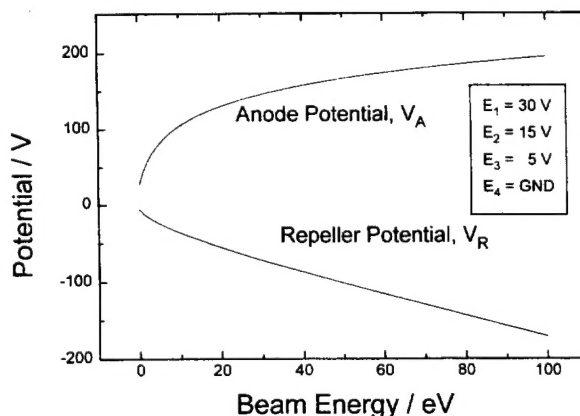


FIG. 4. Anode and repeller potential as a function of the beam energy/cathode potential. The electrode potentials have been kept constant during the optimization process. The curves have been obtained by optimizing the two potentials at different beam energies for constant beam profile and then curve fitting the result.
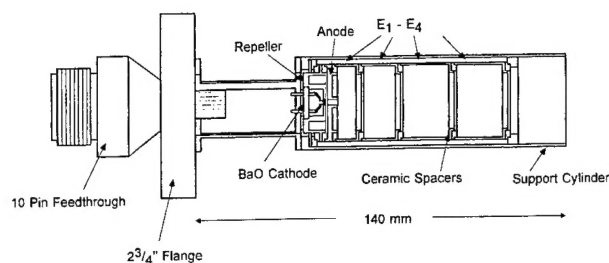
FIG. 5. The design of the low-energy electron gun. The BaO cathode disk and the alumina ceramic spacers are commercially available. The electron gun elements are stacked inside a support cylinder. The whole assembly is supported on a $2\frac{3}{4}$ in. diam flange with a multipin feedthrough.

insulator base, which is of advantage for applications in which the vacuum chamber is brought to atmosphere frequently. The ceramic rings are commercially available.[12] The inside of the gun metal elements have been gold plated electrochemically in order to increase their surface conductivity and keep molecular adsorption low at constant work function.

The trajectory of low-energy electrons is strongly affected by the magnetic field of the earth or other sources. Therefore, the electron gun and the region to the sample should be magnetically shielded.

## III. ELECTRON GUN PERFORMANCE

Figure 6 shows the measured electron current on a grounded aluminum single-crystal sample (crystal diameter 15 mm). A BaO emitter disk was mounted in this case. The beam has been focused for each energy by the use of the electrodes $E_1$–$E_4$ (all at the same potential) and the cathode heating current for maximum emission. The repeller and anode potentials have been kept constant. As can be seen, the output current under optimized conditions increases with

electron energy at a rate of about 0.9 $\mu$A/eV. Figure 6 clearly demonstrates that microamp currents can be achieved at electron energies near 10 eV and below. There, the gun exhibits similar current capabilities to a gun of simpler design.[8]

After gun assembly, it was found that proper operation potentials differed significantly from those employed in trajectory calculations. The reason for this behavior is the location of the cathode disk relative to the repeller. The observed behavior could be explained by moving the cathode disk slightly in the beam direction. After taking this misplacement into account, the calculated potential settings matched the actual operation conditions very well.

## IV. SUMMARY

An electron gun has been designed and built to provide a low-energy, high current, uniform electron flux to a target of a few $cm^2$ surface area. The high electron flux provided allows the study of electron stimulated surface chemistry at low electron excitation energies of a few electron volts. The uniform electron bombardment results in a homogenous surface treatment, and the irradiated surface can then be studied by methods that sample the entire surface area.
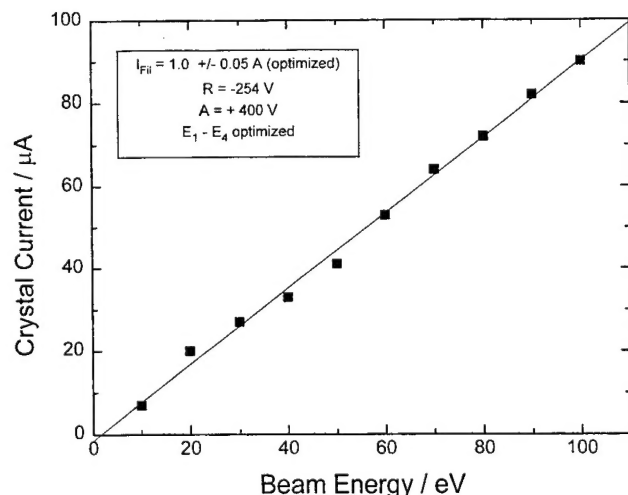
## ACKNOWLEDGMENT

FIG. 6. The current measured at an aluminum single-crystal target when focusing the beam with the electrodes and setting the repeller and anode to high potentials for optimum output. The current is roughly proportional to the beam energy and rises at a rate of about 0.9 $\mu$A/eV.

[1] G. Ertl and J. Küppers, *Low Energy Electrons and Surface Chemistry* (VCH, Weinheim, 1985).

[2] M. P. Seah and W. A. Dench, Surf. Interface Anal. **1**, 2 (1979), and references therein.

[3] H. Ibach and D. L. Mills, *Electron Energy Loss Spectroscopy and Surface Vibrations* (Academic, New York, 1982).

[4] M. J. Edgell, R. W. Paynter, and J. E. Castle, Surf. Interface Anal. **8**, 113 (1986).

[5] For electron gun design and trajectory calculations, see e.g., P. W. Hawkes and E. Kasper, *Principles of Electron Optics* (Academic, New York, 1992).

[6] R. D. Ramsier and J. T. Yates, Jr., Surf. Sci. Rep. **12**, 243 (1991); H. J. Jänsch, J. Xu, and J. T. Yates, Jr., J. Chem. Phys. **99**, 721 (1993).

[7] D. Klyachko, P. Rowntree, and L. Sanche, Surf. Sci. **346**, L49 (1996).

[8] J.-L. Lin and J. T. Yates, Jr., J. Vac. Sci. Technol. A **5**, 2795 (1994).

[9] Idaho National Engineering Laboratory, Chemical Materials & Processes Department, Lockheed Idaho Technologies Company, Idaho Falls, ID 83415; see also, www.srv.net/~klack/simion.html.

[10] Kimball Physics, ES-015 on AEI base, 311 Kimball Hill Rd., Wilton, NH 03086-9742.

[11] V. S. Smentkowski and J. T. Yates, Jr., J. Vac. Sci. Technol. A **12**, 219 (1994); **12**, 224 (1994).

[12] Scientific Instrumentation Services, 1027 Old York Rd., Ringoes, NJ 08551-1039 ($Al_2O_3$ ceramic insulator, Finnigan No. 400005-20070).

# REPORT OF INVENTIONS AND SUBCONTRACTS

(Pursuant to "Patent Rights" Contract Clause) (See Instructions on Reverse Side.)

Public reporting burden for this collection of information is estimated to average 5 minutes per response, including the time for reviewing instructions, searching existing data sources, gathering and maintaining the data needed, and completing and reviewing the collection of information. Send comments regarding this burden estimate or any other aspect of this collection of information, including suggestions for reducing this burden, to Washington Headquarters Services, Directorate for Information Operations and Reports, 1215 Jefferson Davis Highway, Suite 1204, Arlington, VA 22202-4302, and to the Office of Management and Budget, Paperwork Reduction Project (0704-0039), Washington, DC 20503.

| 1a. NAME OF CONTRACTOR/SUBCONTRACTOR | b. CONTRACT NUMBER | 2a. NAME OF GOVERNMENT PRIME CONTRACTOR | c. CONTRACT NUMBER | 3. TYPE OF REPORT (X one) |
|---|---|---|---|---|
| University of Pittsburgh | F49620-93-1-0341 | AFOSR | | a. INTERIM [X]  b. FINAL |
| b. ADDRESS (Include ZIP Code) 3109 Cathedral of Learning Pittsburgh, PA 15260 | d. AWARD DATE (YYMMDD) 1 April 1995 | b. ADDRESS (Include ZIP Code) | d. AWARD DATE (YYMMDD) | 4. REPORTING PERIOD (YYMMDD) a. FROM 9/31/96  b. TO 10/10/97 |

## SECTION I – SUBJECT INVENTIONS

5. "SUBJECT INVENTIONS" REQUIRED TO BE REPORTED BY CONTRACTOR/SUBCONTRACTOR (If "None," so state)

| a. NAME(S) OF INVENTOR(S) (Last, First, MI) | b. TITLE OF INVENTION(S) | c. DISCLOSURE NO., PATENT APPLICATION SERIAL NO. OR PATENT NO. | d. ELECTION TO FILE PATENT APPLICATIONS | | | | | e. CONFIRMATORY INSTRUMENT OR ASSIGNMENT FORWARDED TO CONTRACTING OFFICER | |
|---|---|---|---|---|---|---|---|---|---|
| | | | (1) United States | | (2) Foreign | | | (1) Yes | (2) No |
| | | | (a) Yes | (b) No | (a) Yes | (b) No | | | |
| NONE | "Method for Fluorination of Diamond Surfaces and Associated Product" | 08/798311 | X | | | X | | | X |
| | "An Improved Method for Lubrication of Diamond Like Carbon Surfaces" | 08/764392 | X | | | X | | | X |

f. EMPLOYER OF INVENTOR(S) NOT EMPLOYED BY CONTRACTOR/SUBCONTRACTOR

| (1)(a) Name of Inventor (Last, First, MI) | (2)(a) Name of Inventor (Last, First, MI) |
|---|---|
| J.T. Yates, Jr. | V.S. Smentkowski |
| (b) Name of Employer | (b) Name of Employer |
| Univ. of Pittsburgh | Univ. of Pittsburgh |
| (c) Address of Employer (Include ZIP Code) | (c) Address of Employer (Include ZIP Code) |
| Pittsburgh, PA 15260 | Pittsburgh, PA 15260 |

g. ELECTED FOREIGN COUNTRIES IN WHICH A PATENT APPLICATION WILL BE FILED

| (1) Title of Invention | (2) Foreign Countries of Patent Application |
|---|---|

## SECTION II – SUBCONTRACTS (Containing a "Patent Rights" clause)

6. SUBCONTRACTS AWARDED BY CONTRACTOR/SUBCONTRACTOR (If "None," so state)

| a. NAME OF SUBCONTRACTOR(S) | b. ADDRESS (Include ZIP Code) | c. SUBCONTRACT NO(S) | d. DESCRIPTION OF WORK TO BE PERFORMED UNDER SUBCONTRACT(S) | | e. SUBCONTRACT DATES (YYMMDD) | |
|---|---|---|---|---|---|---|
| | | | (1) Clause Number | (2) Date (YYMM) | (1) Award | (2) Estimated Completion |
| NONE | | | | | | |

## SECTION III – CERTIFICATION

7. CERTIFICATION OF REPORT BY CONTRACTOR/SUBCONTRACTOR (Not required if: Small Business or Nonprofit organization) (X appropriate box)

c. I certify that the reporting party has procedures for prompt identification and timely disclosure of "Subject Inventions," that such procedures have been followed and that all "Subject Inventions" have been reported.

| a. NAME OF AUTHORIZED CONTRACTOR/SUBCONTRACTOR OFFICIAL (Last, First, MI) | b. TITLE | c. SIGNATURE | d. DATE SIGNED |
|---|---|---|---|
| Correa, Caroline | Assistant Controller | Carline Correa | 10/9/97 |

DD Form 882, OCT 89    ET/ 5-36963    Previous editions are obsolete

[54] **METHOD FOR FLUORINATION OF DIAMOND SURFACES**

[75] Inventors: **Vincent S. Smentkowski**, Pittsburgh; **John T. Yates, Jr.**, Allison Park, both of Pa.

[73] Assignee: **University of Pittsburgh of the Commonwealth System of Higher Education**, Pittsburgh, Pa.

[56] **References Cited**

PUBLICATIONS

Smentkowski et al, Mater. Res. Soc. Symp. Proc., 416 (Diamond for Electronic Applications), 293–8 1996 (Abstract) Smentkowski et al, Science, 271 (5246), 193–5, 1996.

P. Cadman et al., "Identification of Functional Groups on the Surface of a Fluorinated Diamond Crystal by Photoelectron Spectroscopy," *J.C.S. Chem. Comm.*, pp. 654–655, 1975.

*CRC Handbook of Chemistry and Physics*, CRC Press, Boca Raton, Florida, part 63 Edition, pp. 196–202, 1982–1983.

J.E. Field, "The Properties of Diamond," Academic, New York, New York 1979 (reference book only). No Page Number.

J.F. Morar et al., "C 1 s excitation studies of diamond (111). I. Surface core levels," *The American Physical Society*, Physical Review B, vol. 33, No. 2, pp. 1340–1345, Jan. 15, 1986.

J.F. Morar et al., "C 1 s excitation studies of diamond (111). II. Unoccupied surface states," *The American Physical Society*, Physical Review B, vol. 33, No. 2, pp. 1346–1349, Jan. 15, 1986.

P.K. Bachmann et al., "Emerging Technology of Diamond Think Films," *Chemical and Engineering News*, vol. 67, No. 20, pp. 24–39, May 15, 1989.

Donald E. Patterson et al., "Fluorinated Diamond Films, Slabs, and Grit," *Materials Research Society Symposium Proceedings*, vol. 140, pp. 351–356, 1989.

David S.Y. Hsu et al., "Fluorination of Diamond(111) Single Crystal Surfaces By XeF$_2$," *Fourth SDIO/IST ONR Diamond Technology Initiative Symposium*, Jul. 1989. No Page Number.

Robert Pool, "Diamond Films Sparkle As They Come to Market," *Science*, vol. 249, No. 4964, pp. 27–28, Jul. 6, 1990.

Barnaby J. Feder, "Industry's Growing Romance With Diamonds," *The New York Times*, Feb. 21, 1990, p. D5.

Daniel E. Koshland, Jr., "The Molecule of the Year," *Science*, vol. 250, No. 4988, Dec. 21, 1990. p. 1637.

Andrew Freedman et al., "Fluorination of diamond (100) by atomic and molecular beams," *Appl. Phys. Lett.*, vol. 57, No. 12, Sep. 17, 1990, pp. 1194–1196.

Andrew Freedman et al., "Fluorination of Diamond (100) By Atomic And Molecular Beams," *New Diamond Science and Technology*, MRS Int. Conf. Proc., vol. 2, pp. 321–236, Sep. 23–27, 1990.

J.E. Field, "The Properties of Natural and Synthetic Diamonds," *Academic*, New York, New York (1992). No Page Number (Reference book.)

S.K. Ritter, "Fluorine Chemistry Branches Out From Its Traditional Focus,", *Chemical and Engineering News*, vol. 73, No. 9, Feb. 27, 1995. pp. 39–44.
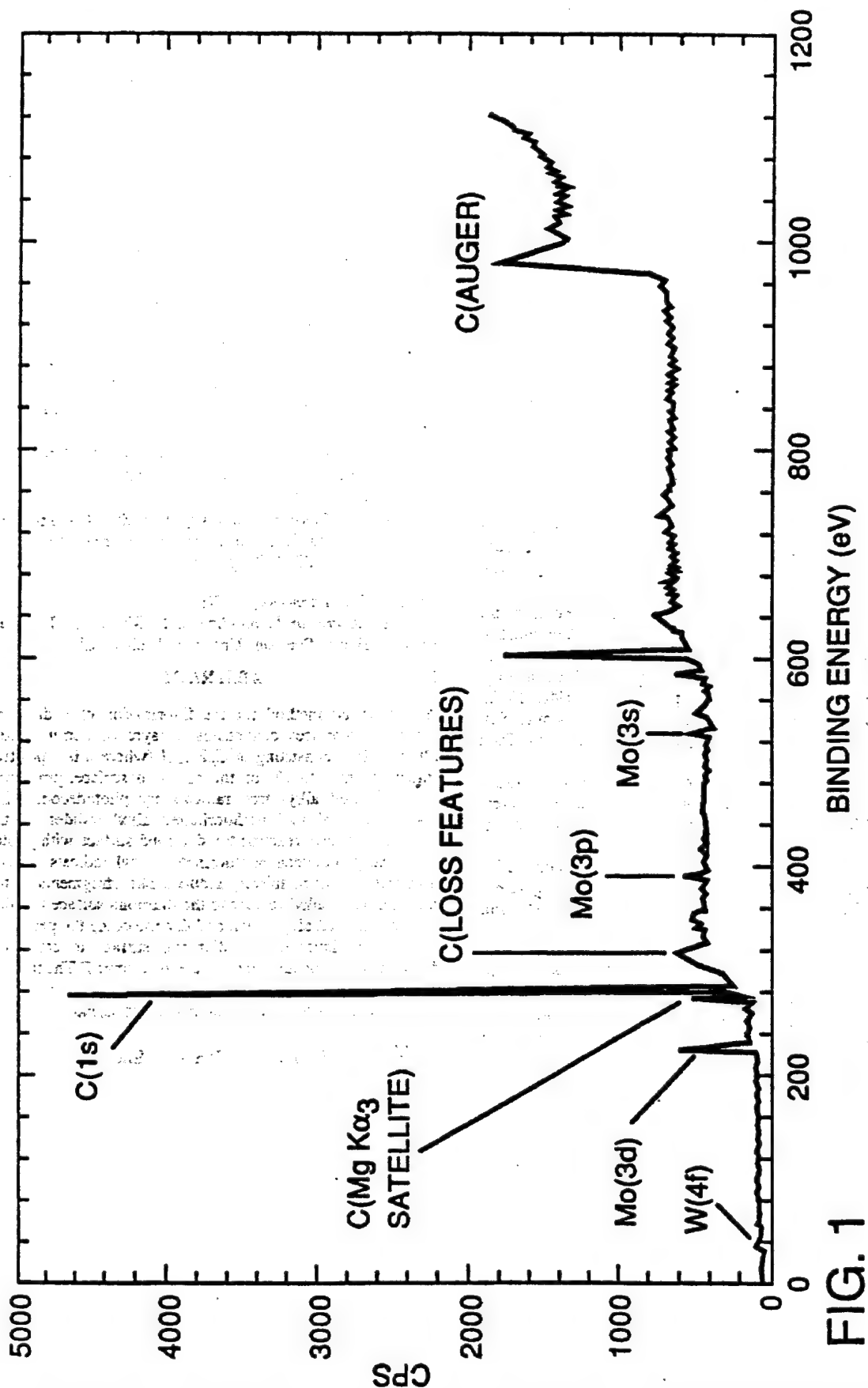
[57] **ABSTRACT**

An improved method for the fluorination of a diamond surfaces comprises condensing a layer of perfluorinated alkyl iodides consisting of $C_nF_{2n+1}I$ (where n is a positive integer from 1 to 13) on the diamond surface, producing perfluorinated alkyl free radicals by photodecomposing C—I bonds of said perfluorinated alkyl iodides on the diamond surface, reacting the diamond surface with photochemically produced perfluorinated alkyl radicals thereby anchoring photochemically induced photofragments of the perfluorinated alkyl iodides to the diamond surface forming a perfluorinated alkyl layer, and decomposing the perfluorinated alkyl layer on the diamond surface to cause the fluorination of the diamond surface by atomic F. The method achieves greater than one fluorine atom per surface carbon atom chemisorbed on the diamond using $C_4F_9I$.

**8 Claims, 11 Drawing Sheets**

FIG. 1

$C_4F_9I$ EXPOSURE = 5 X 10$^{16}$cm$^{-2}$ AT 119K

DIAMOND HEATED TO 300 K FOLLOWING IRRADIATION AND PRIOR TO XPS ANALYSIS
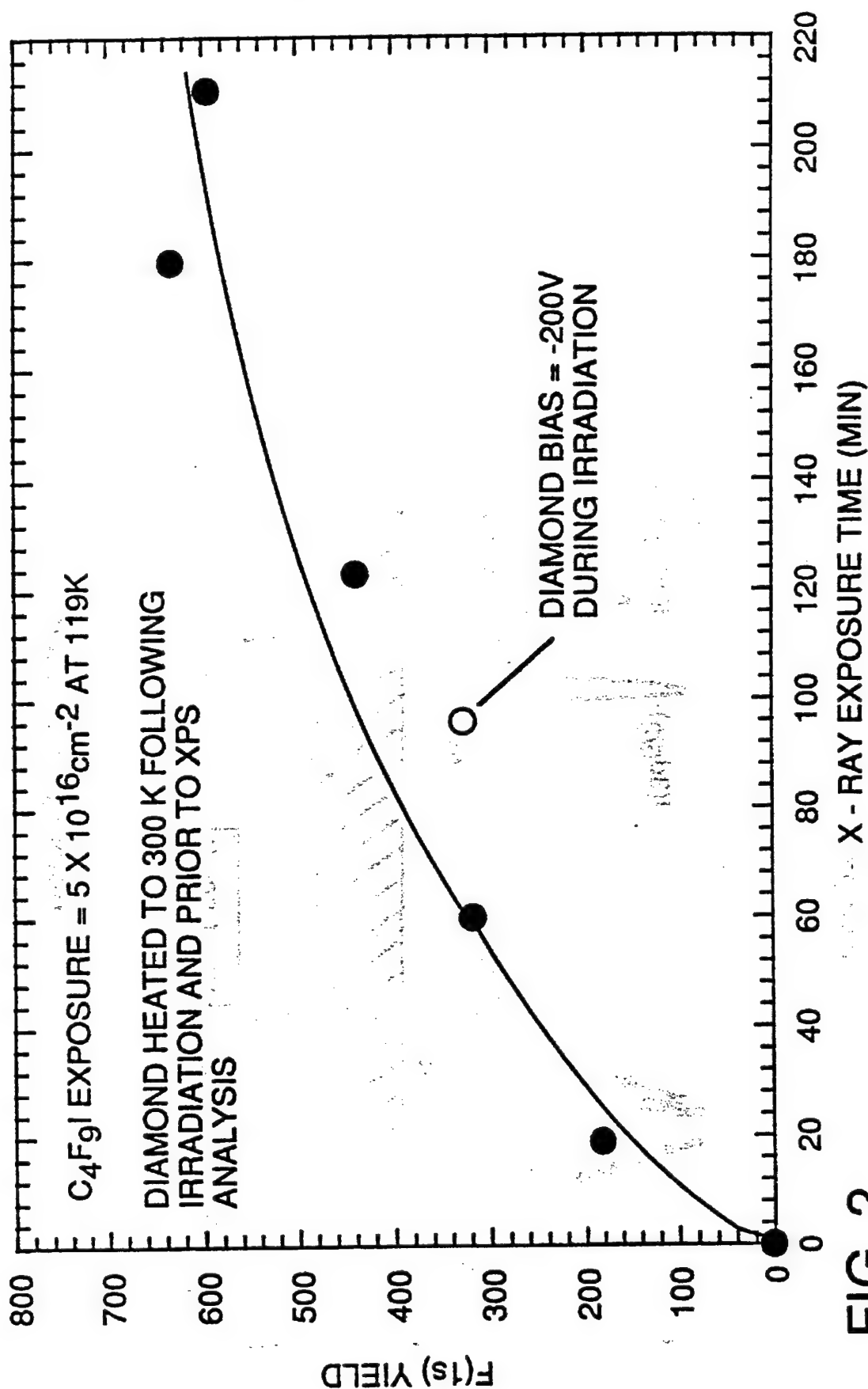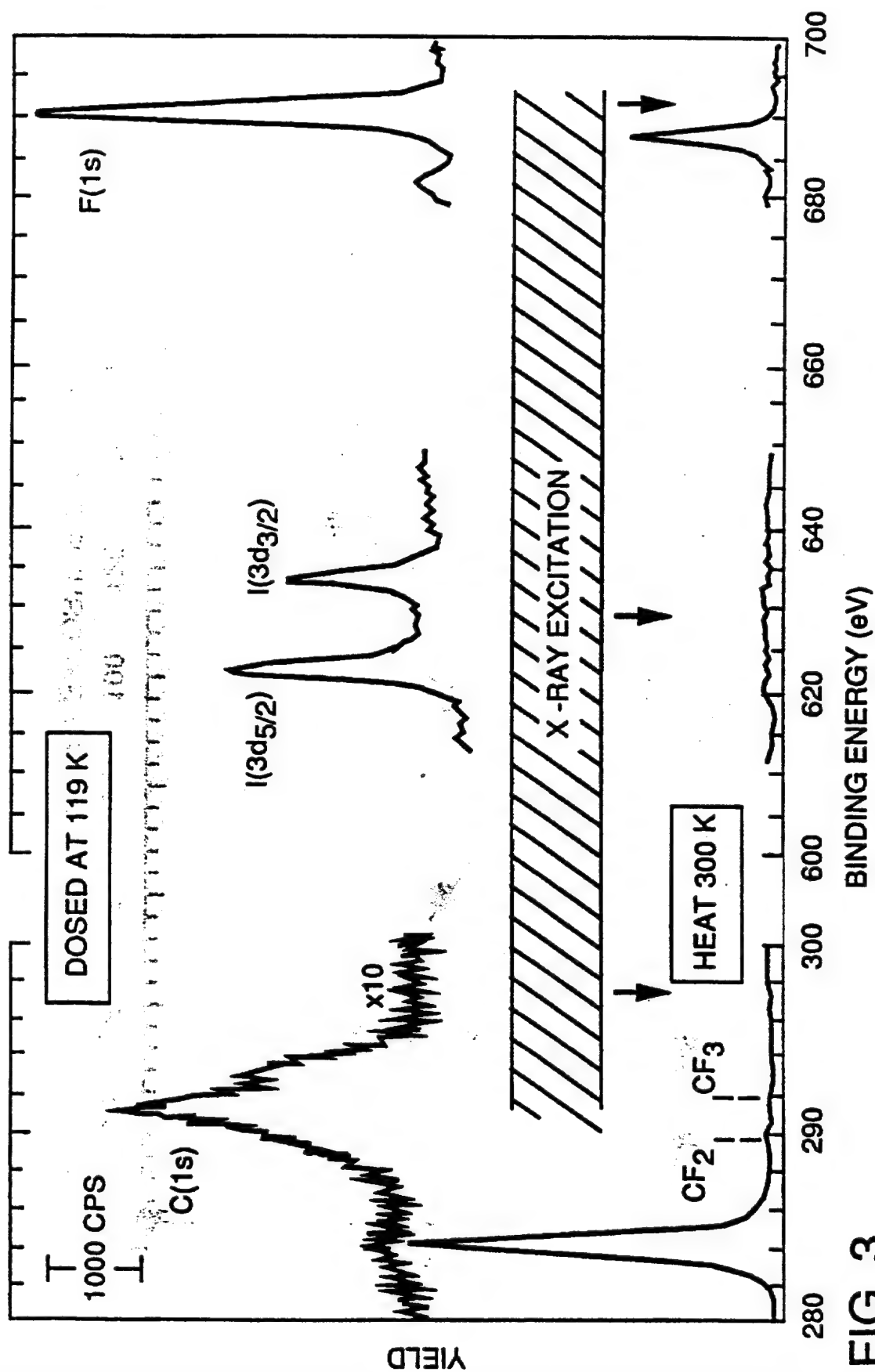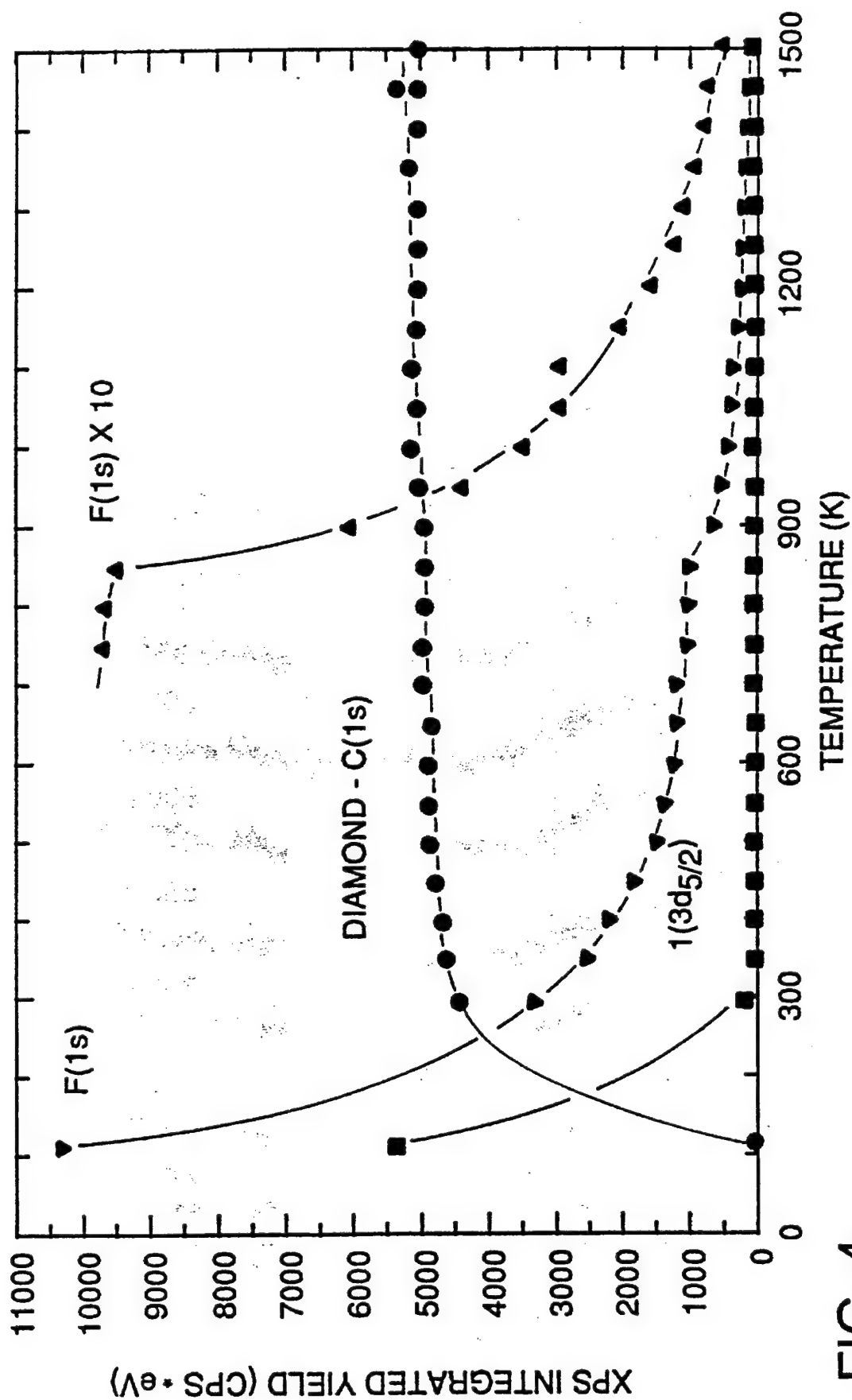
DIAMOND BIAS = -200V DURING IRRADIATION

X - RAY EXPOSURE TIME (MIN)

F(1s) YIELD

FIG. 2

FIG. 3

FIG. 4

FIG. 5

FIG. 6

FIG. 7
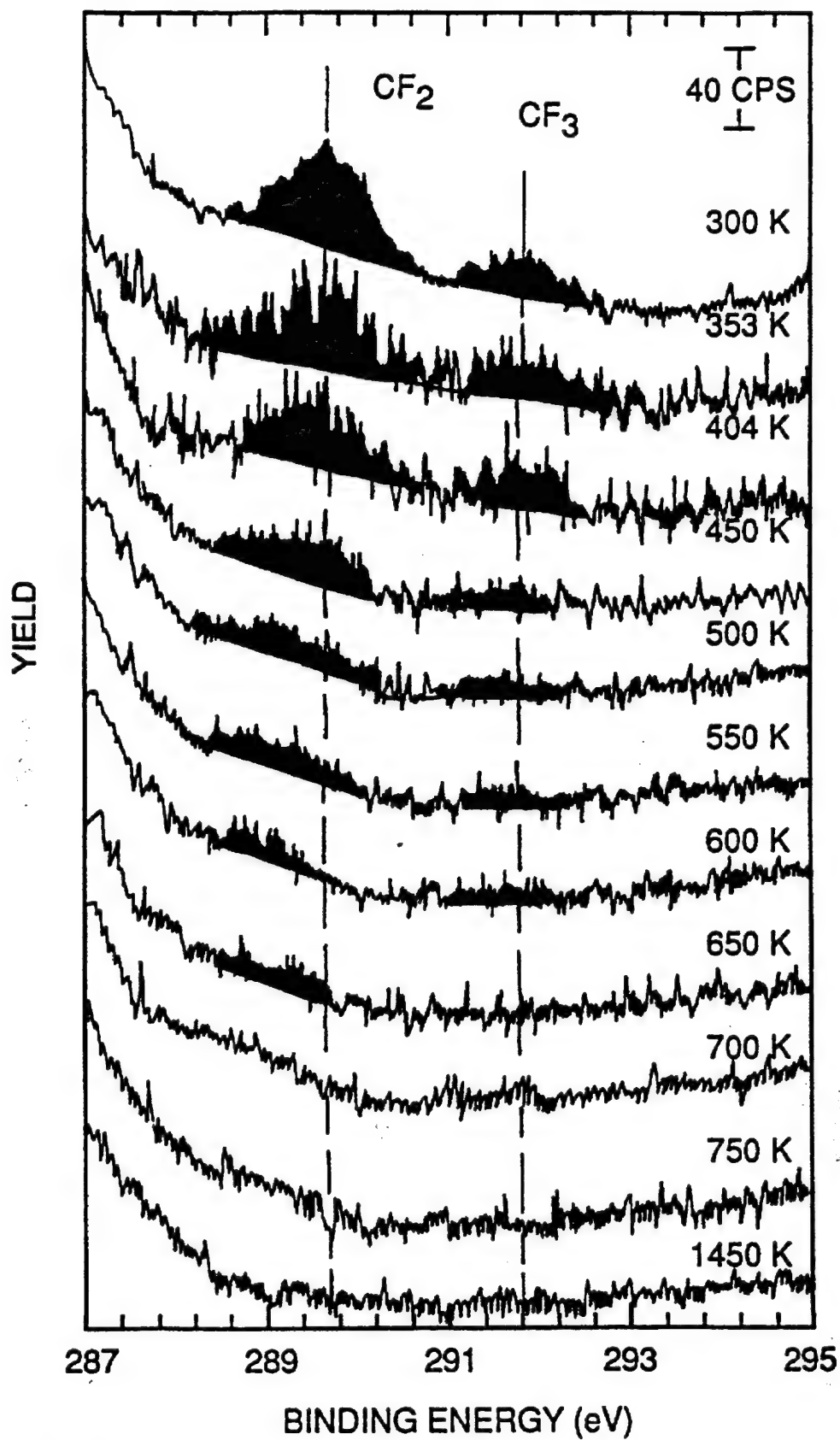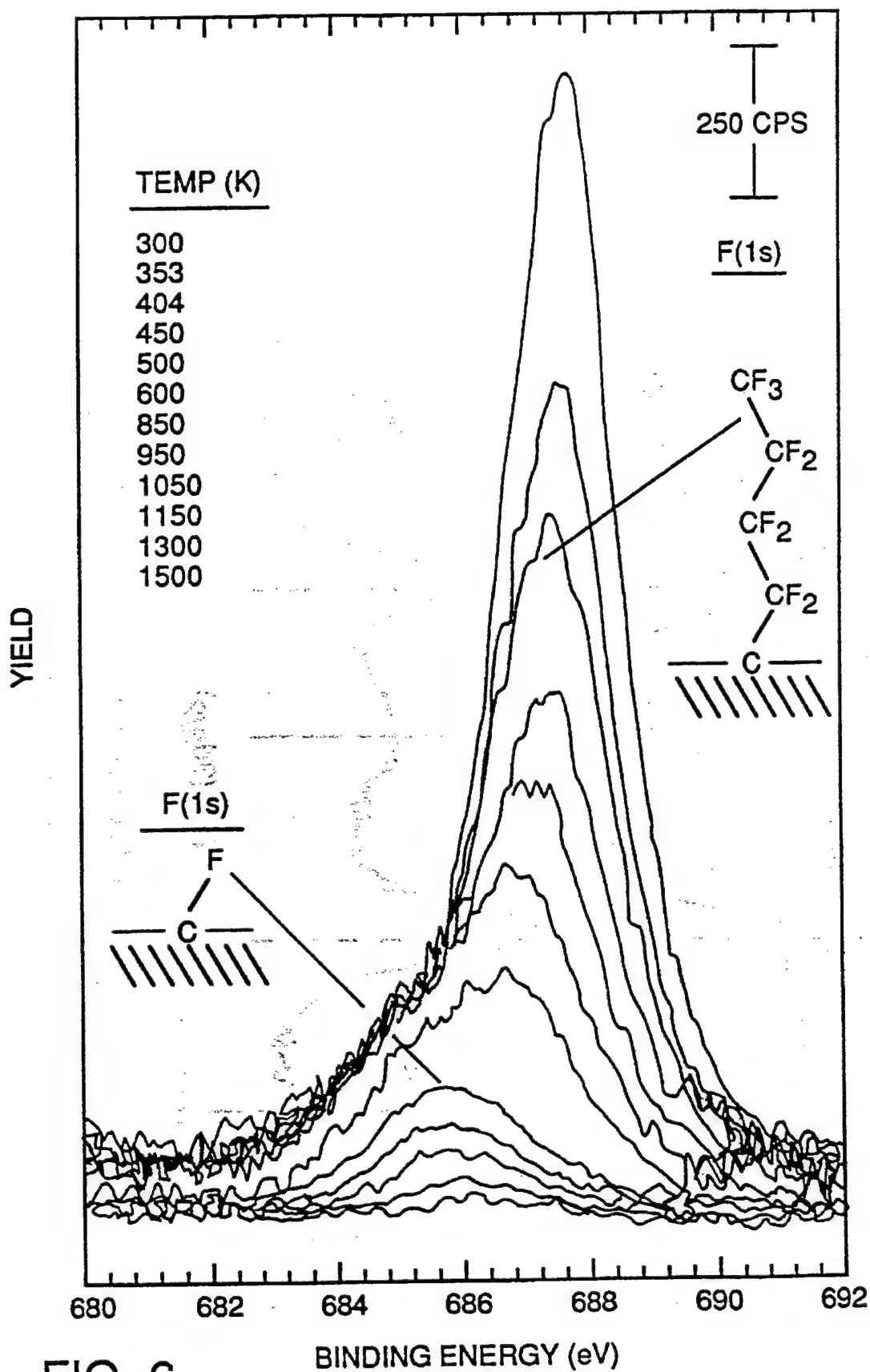
FIG. 8C



FIG. 8B



FIG. 8A
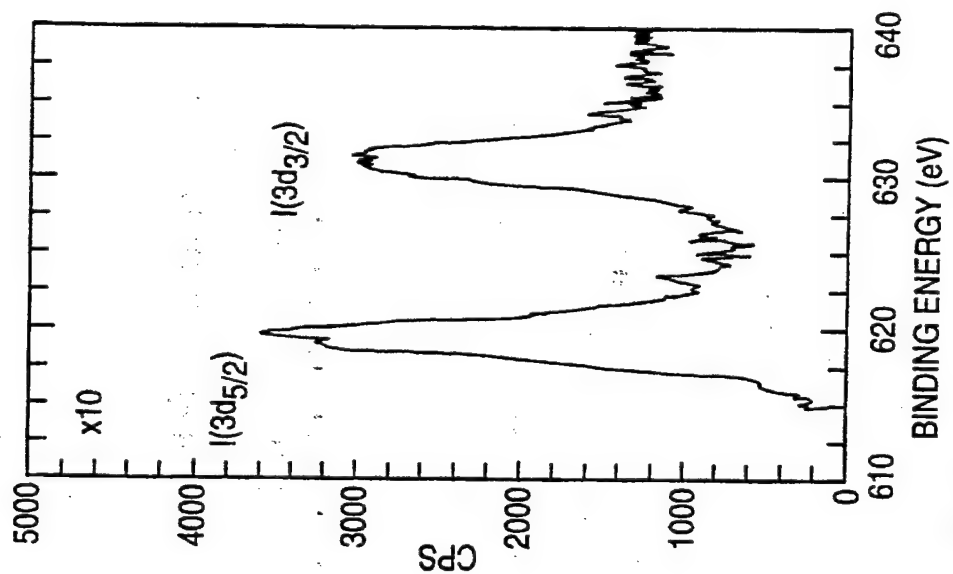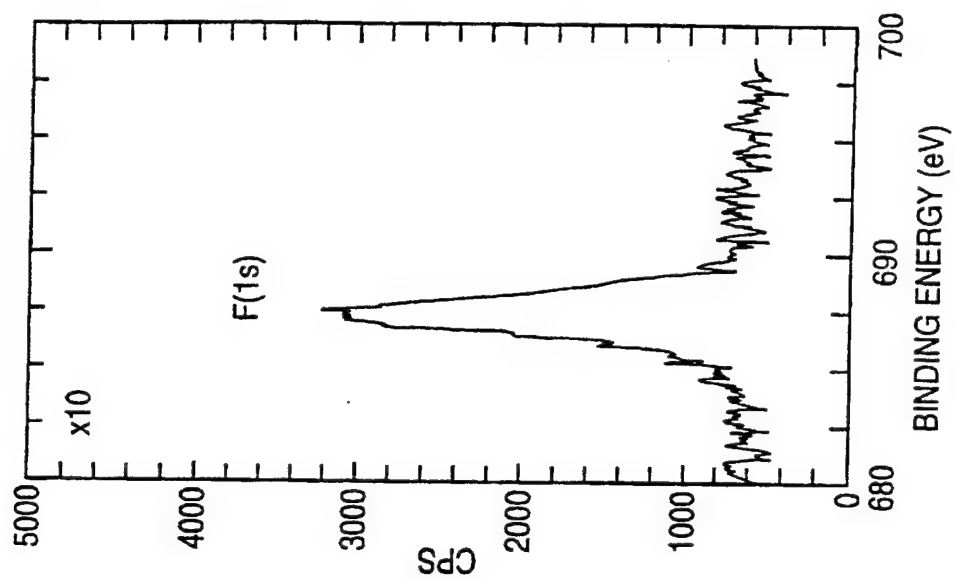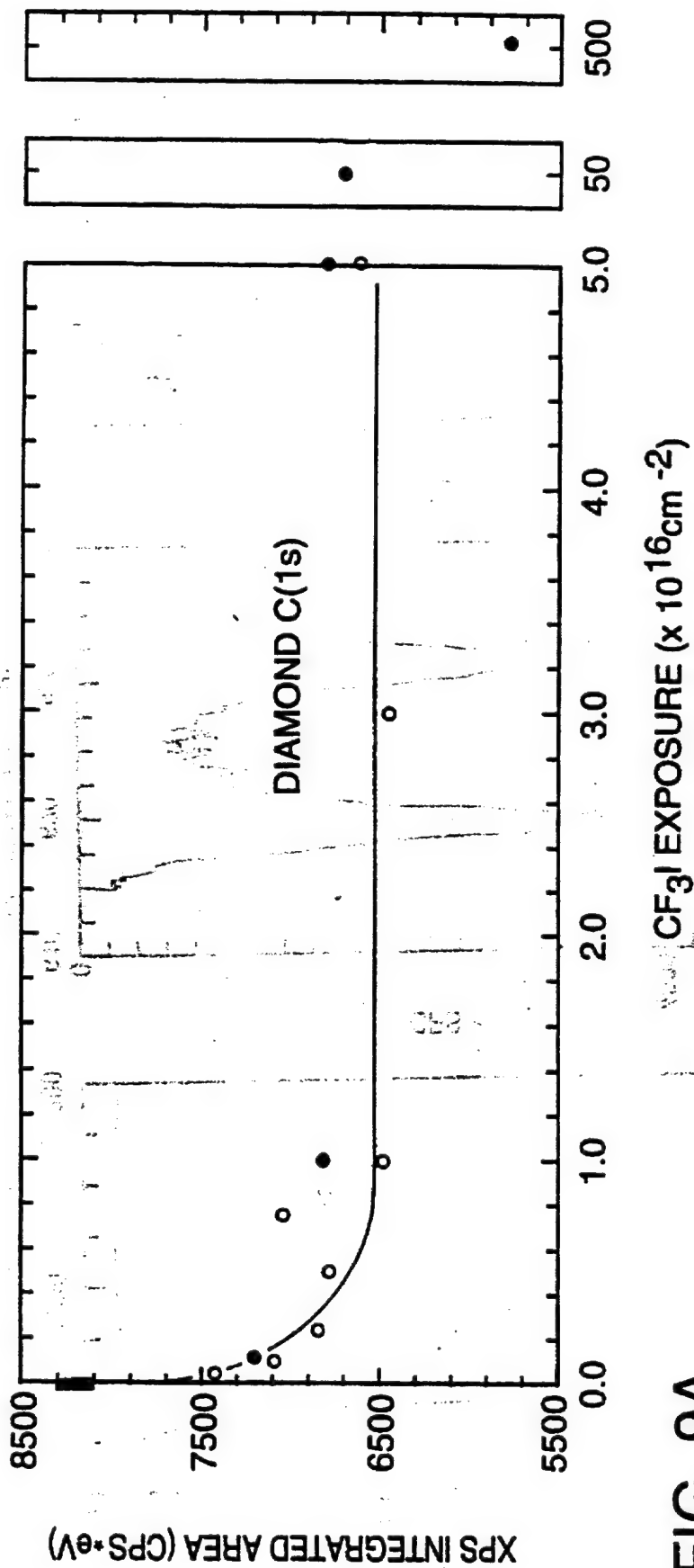
FIG. 9A
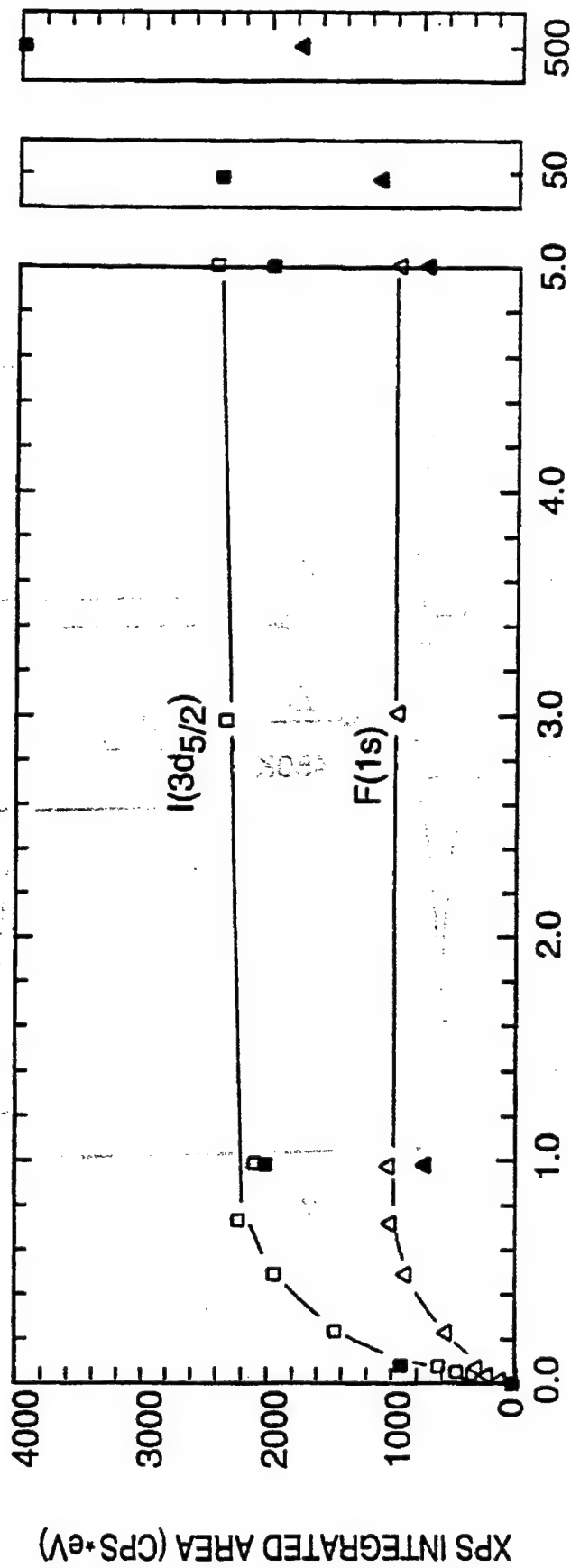
FIG. 9B

FIG. 10
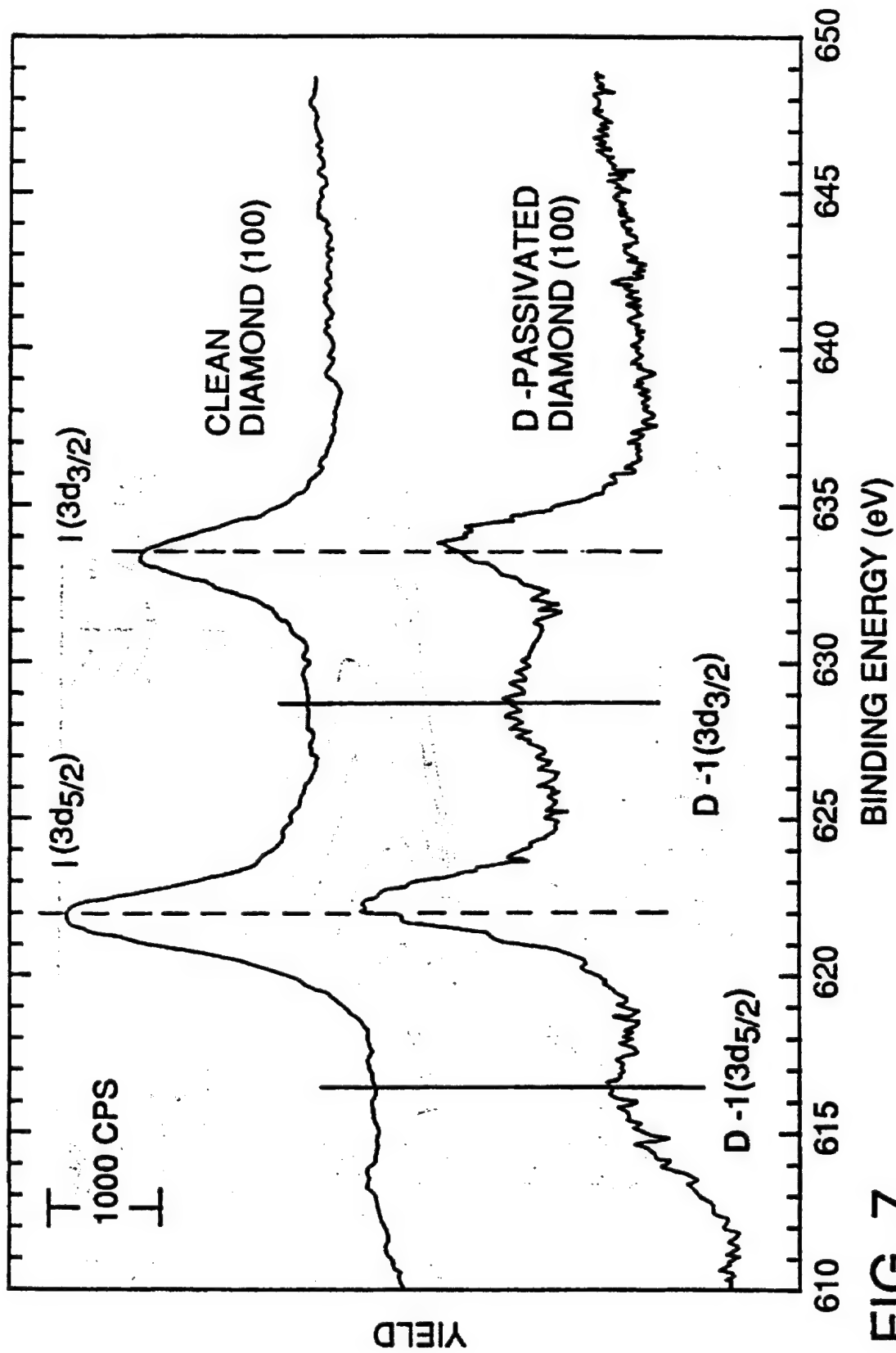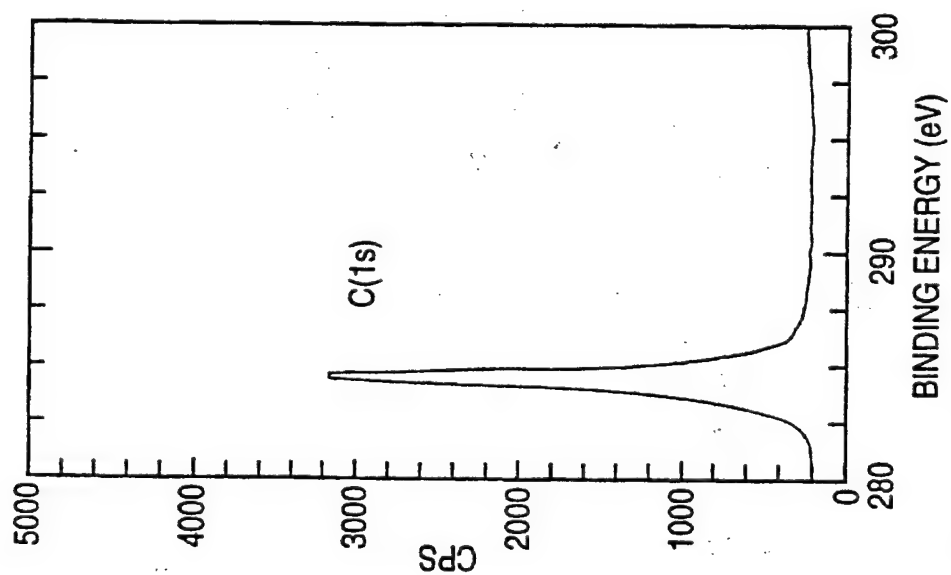
# METHOD FOR FLUORINATION OF DIAMOND SURFACES

## BACKGROUND OF THE INVENTION

### 1. Field of the Invention

The present invention relates to the photodecomposition of all perfluoroalkyl iodides of general formula $C_nF_{2n+1}I$ (where n is a positive integer from 1 to 13) on diamond surfaces as an improved method of fluorination of a diamond surface. This invention also relates to using $C_nF_{2n+1}I$ molecules as photochemically activated fluorinating agents, photodecomposing the fluoroalkyl iodide molecule, attachment of the photofragments to the diamond surface and thermal decomposition of the fluoroalkyl ligands. The fluorinated layer produced by 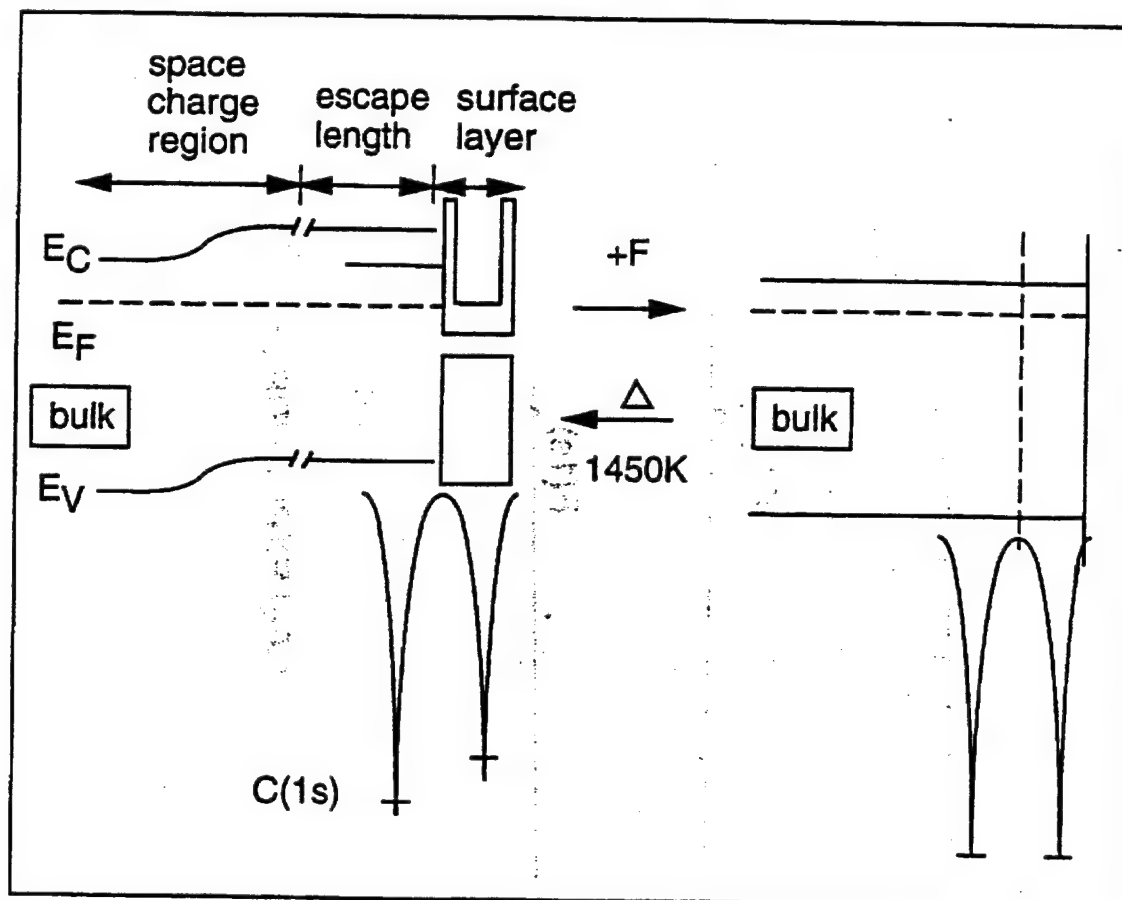this new method has been found to exhibit high thermal stability, comparable to surface layers produced by direct fluorination of diamond with F atoms. A fluorinated diamond surface is made by the disclosed method.

### 2. Description of the Prior Art

The surface properties of many materials may be significantly improved by the use of diamond film coatings. Diamond films exhibit physical properties making possible the fabrication of long-lived cutting tools, biological implants, optical disks, lenses and windows. [P. K. Bachmann et at., *Chemical Engineering News*, 67 (20), 24 (1989); J. E. Field, "The Properties of Diamonds", Academic, New York (1979); J. E. Field, "The Properties of Natural and Synthetic Diamonds", Academic, New York (1992); R. Pool. *Science*, 249, 27 (1990); B. J. Feder, *The New York Times*, Feb. 21, 1990, p. C4; D. E. Koshland, Jr., *Science*, 250, 1637 (1990).] In each of these applications, it is desirable to modify the properties of the outer surface of the diamond film itself in order to build in special surface properties of the protective diamond coating.

The chemical modification of diamond surfaces provides one route for producing useful surface properties. One modifier which offers promise for the improvement of the behavior of diamond surfaces is fluorine. [S. K. Ritter, *Chemical and Engineering News*, 73 (9), 39 (1995).] It has been shown that the strong surface C—F bonds [*Handbook of Chemistry and Physics*, CRC Press, Boca Raton, Fla. (1982–83), 63 Edition, p. F-199] on diamond provide enhanced lubricity [D. S. Y. Hsu et al., *Fourth SDIO/IST ONR Diamond Technology Initiative Symposium*, July 1989] and enhanced stability under oxidizing conditions at elevated temperatures [D. E. Patterson et al., *Mat. Res. Soc. Symp. Proc.*, 140, 351 (1989)].

Until now, the fluorination of diamond surfaces has been accomplished only with extreme surface treatment methods involving molecular $F_2$, atomic F [A. Freedman et al., *Appl. Phys. Lett.*, 57, 1194 (1990); *Mat. Res. Soc. Symp. Proc.*, 204, 571 (1991); *Proc. Electrochem. Soc.*, 91, 494 (1991); *New Diamond Sci. Technol., Proc. Internat. Conf.*, 2, 321 (1991)], $XeF_2$ [J. F. Morar et al., *Phys. Rev. B.*, 33, 1340 (1986); J. F. Morar et al., *Phys. Rev. B.*, 33, 1346 (1986)], and fluorine-containing plasmas [P. Cadman et al., *J. Chem. Soc. Chem. Comm.*, 654 (1975)]. Each of these surface modification methods involves handling corrosive gases under harsh treatment conditions. In addition, only partial fluorination of the diamond surfaces studied has been achieved using these extreme methods. To the best of the Applicants' knowledge, no one to date has reported the attachment of long chain fluoroalkyl species to diamond surfaces.

In spite of previous methods involving elemental $F_2$, atomic F, plasmas containing fluorine species and $XeF_2$,

materials which are hard to handle and need special techniques, there still remains a need for an improved method which provides an improved chemical reaction route for producing a fluorinated diamond surface which is stable to high temperatures.

## SUMMARY OF THE INVENTION

The present invention has met the above-described need. The present invention provides a method of using all perfluorinated alkyl iodides ($C_nF_{2n+1}I$) where n is a whole integer from 1 to 13 for producing a fluorinated diamond surface.

The improved method for the fluorination of a diamond surface comprises depositing a layer of perfluorinated alkyl iodides consisting of $C_nF_{2n+1}I$ molecules (where n is from 1 to 13) on the diamond surface, producing perfluorinated alkyl radicals by photodecomposing the C—I bonds of the perfluorinated alkyl iodide on the diamond surface and reacting the diamond surface with the photochemically produced perfluorinated alkyl radicals. The photochemically induced photofragments of the perfluorinated alkyl iodide molecules are anchored to the diamond surface forming a perfluorinated alkyl layer and the fluorinated alkyl layer is decomposed on the diamond surface to produce chemisorbed fluorine on the diamond surface. The method achieves greater than one fluorine atom per surface carbon atom on the diamond surface. The method produces thermally stable chemisorbed fluorine on the diamond surface. Following photodecomposition of the perfluoroalkyl iodide on the diamond surface, heating from about 120K to 300K to desorb excess perfluoroalkyl iodide on the diamond surface, and then employing a temperature of about 300K to 700K to decompose the perfluoroalkyl layer, a layer of chemisorbed fluorine is produced on the diamond surface.

A fluorinated diamond is made by the above method selecting the perfluorinated alkyl iodide, $C_nF_{2n+1}I$, selected from the group consisting of wherein n=1 to 5.

Attachment of fluorine to the diamond surface, using $C_4F_9I$ as a representative starting material, is characterized by band bending as surface states on the diamond are occupied through chemisorption and this results in shifting of the C(1s) level as measured by X-ray photoelectron spectroscopy. The iodine on the diamond surface is removed by heating from about 120K to 400K. A chemisorbed $C_4F_9$ surface species is stable from about 120K to 500K and then decomposes to produce chemisorbed fluorine on the diamond. The chemisorbed fluorine remains stable on the diamond surface from about 500K to about 1500K, preferably 700K to 1500K. The fluorinated diamond surface has thermal stability to 1500K. The same surface chemistry occurs on hydrogen-passivated diamond and HI species are detected following irradiation of $C_4F_9I$.

It is an object of this invention to provide an improved method for the fluorination of diamond surfaces using radiation-induced or ultraviolet light-induced activation of perfluoroalkyl iodide molecules adsorbed on the diamond surface to produce perfluoroalkyl groups chemically bound to the diamond.

It is an object of this invention to provide a method wherein the anchored fluoroalkyl groups are an easily controlled source of fluorine for the production of chemisorbed fluorine on the diamond surface, by subsequent thermal decomposition.

It is an object of this invention to provide a method and product wherein the presence of passivating surface C—H groups on the diamond does not inhibit fluorination by this method.

3

It is an object of the present invention to provide a method and a product where fluorinated diamond surfaces have a low coefficient of friction.

It is an object of this invention to provide an improved method and product wherein there is enhanced diamond resistance to oxidation by $O_2$ and atomic O.

It is another object of this invention to provide a new method and product wherein the fluorinated layer on a diamond surface exhibits high thermal stability.

It is another object of this invention to provide a method and product wherein fluorinated layers produced by the present invention have comparable properties to layers produced by direct fluorination of the diamond with F atoms.

It is yet another object of this invention to provide an improved new method and product wherein more than one fluorine atom is deposited per surface carbon atom on the diamond.

These and other objects of the invention will be more fully understood from the following description of the invention and references to the illustrations and appended claims hereto.

## BRIEF DESCRIPTION OF THE DRAWINGS

FIG. 1 shows broad scan X-ray photoelectron spectroscopy (XPS) of the clean diamond obtained following heating to 1450K.

FIG. 2 is a plot of F(1s) yield from chemically-bound F as a function of X-ray exposure time for $C_4F_9I$ layers on diamond (100) at about 119K.

FIG. 3 shows XP spectra of $C_4F_9I$ on diamond (100) at about 119K (top), and the transformation which occurs following irradiation and heating to about 300K.

FIG. 4 is a plot of the thermal behavior of a $C_4F_9I$ layer on diamond (100) following irradiation and heating up to elevated temperatures.

FIG. 5 shows changes in $CF_2$— and $CF_3$—XPS features from anchored $C_4F_9$ species following X-irradiation and upon heating.

FIG. 6 shows changes in F(1s) XPS intensity as a function of heating following $C_4F_9I$ irradiation.

FIG. 7 is an XP spectra of the I(3d) region following X-irradiation of the $C_4F_9I$ layer on a hydrogen-passivated diamond surface.

FIG. 8 shows XP spectra of the C(1s), I(3d), and F(1s) regions following a $CF_3I$ exposure of $5\times10^{16}$ cm$^{-2}$ at about 119K.

FIG. 9 is a plot of the C(1s) [circles], I(3d$_{5/2}$) [squares] and F(1s) [triangle] XPS integrated intensity as a function of $CF_3I$ exposure at about 119K.

FIG. 10 is the effect of band bending for fluorination (and defluorination via heating) of diamond (100).

## DESCRIPTION OF THE PREFERRED EMBODIMENT

The present invention presents an improved method of fluorinating a diamond surface which is capable of depositing more than one fluorine atom per surface carbon atom on the diamond. The fluorinated alkyl layer achieved by this method decomposes between about 300K and 700K to produce a highly stable form of chemisorbed fluorine on the diamond surface which is thermally stable from about 500K to 1500K, preferably about 700 to 1500K. The fluorinated diamond surface has thermal stability to 1500K.

The improved method for the fluorination of a diamond surface comprises depositing a layer of perfluorinated alkyl

4

iodides consisting of $C_nF_{2n+1}I$ (where n is a positive integer 1 to 13) on the diamond surface, producing perfluorinated alkyl radicals by photodecomposing the C—I bonds of the perfluorinated alkyl iodides on the diamond surface and reacting the diamond surface with the photochemically produced perfluorinated alkyl radicals. The photochemically induced photofragments of the perfluorinated alkyl iodide molecules are anchored to the diamond surface forming a perfluorinated alkyl layer and this layer is decomposed on the diamond surface to produce chemisorbed fluorine on the diamond surface. The method produces more than one fluorine atom per surface carbon atom on the diamond surface. The method also produces thermally stable chemisorbed fluorine on the diamond surface. The method employs perfluorinated alkyl iodides $C_nF_{2n+1}I$ selected from the group wherein n=1 to 5 increasing the fluorination of the diamond surface as the size of the perfluoroakyl iodide molecules increases. For n=4 the method also employs the photodecomposition of the perfluoroalkyl iodide on the diamond surface, heating from 120K to 300K to desorb excess perfluoroalkyl iodide on the diamond surface, employing a temperature of about 300K to 700K to decompose the perfluorinated alkyl layer to produce the chemisorbed fluorine on the diamond surface. Simultaneously, iodine atoms from the perfluoroalkyl groups extract hydrogen atoms from the diamond surface making surface sites available for perfluoroalkyl group attachment.

A fluorinated diamond was made by the above method selecting the fluorination perfluoroalkyl iodide from the group consisting of $CF_3I$, $C_2F_5I$, $C_3F_7I$, $C_4F_9I$, $C_5F_{11}I$, $C_6F_{13}I$, $C_7F_{15}I$, $C_8F_{17}I$, $C_9F_{19}I$, $C_{10}F_{21}I$, $C_{11}F_{23}I$, $C_{12}F_{25}I$ and $C_{13}F_{27}I$. The fluorinated diamond was made using the perfluoroalkyl iodide $C_4F_9I$. The fluorinated diamond was also made using the fluorinating perfluoroalkyl iodide $CF_3I$.

Attachment of fluorinated groups to the diamond surface is characterized by band bending as surface states on the diamond are occupied through chemisorption. The C(1s) binding energy of the fluorinated diamond increases indicating removal of surface states on the diamond by chemisorbed fluorine. For n=4 the iodine on the diamond surface is removed by heating from about 120K to 400K. The chemisorbed $C_4F_9$ surface species is stable from about 120K to 300K and then produces chemisorbed fluorine on the diamond over the temperature range 300K to 700K. The chemisorbed fluorine remains stable on the diamond surface from about 500K to 1500K, preferably about 700K to 1500K. The fluorinated diamond surface has thermal stability to 1500K.

## EXAMPLE

The two polished natural diamond (100) crystals (diamond #1 (D#1) and diamond #2 (D#2)); type II a, 6 mm×6 mm×0.5 mm) used in this work have been oriented to within 1° of the (100) orientation. Prior to mounting and insertion into the vacuum system, the crystals were cleaned using accepted wet chemical cleaning procedures. The diamond crystals were indirectly heated by contact with a Mo support can containing a shielded W heating filament which heats the crystal/support assembly either by radiation or by electron bombardment (to >1450K). The temperature of the diamond crystals was accurately measured using two independent W26%Re vs. W5%Re thermocouples which were internally mounted inside the diamond inside laser drilled holes which enter the 0.5 mm thick crystal edges. The maximum deviation between the two diamond thermocouples was 15K at 1450K.

The base pressure in the ultrahigh vacuum system was $\sim1\times10^{-10}$ Torr with a working pressure of $\sim3\times10^{-10}$ Torr.

The diamond was cleaned by heating in vacuum to 1450K (two times), following cycles of atomic D adsorption and desorption. Conditioning of the diamond crystal in atomic D was carried out in a high pressure cell which was isolated from the UHV analysis chamber by a gate valve. Atomic D exposures were made using a hot W filament (~1800K) in $D_2(g)$ with line-of-sight geometry to the diamond (100) crystal. Reproducible C(1s) binding energies, integrated C(1s) yields, and constant C(1s) line widths were achieved in this manner. It has been shown that irreproducible surfaces may result for other diamond surface preparation procedures.

A broad scan XP spectrum of diamond (100) following conditioning in atomic D and cleaning at 1450K is shown in FIG. 1. The spectrum (and expanded regions of the spectrum—not shown) indicate that neither graphite nor surface oxygen impurities are present. Previous studies indicate that chemisorbed D is also absent following heating to 1450K. Mo features from the Mo support are seen as well as small W features from the thermocouples.

Exposure of the diamond (100) crystal to an effusive beam of $C_4F_9I(g)$ or $CF_3I(g)$ was achieved in the ultrahigh vacuum system by reproducibly bringing the diamond crystal to within 4 mm of a 5 mm×5 mm orifice which accurately delivers the fluoroalkyl iodide beam to the diamond. The flow rate was governed by a nominal 2 μ diameter pinhole in the gas delivery system, using a Baratron capacitance manometer for measuring the backing pressure. Absolute fluoroalkyl iodide fluxes were calculated using effusion measurements for $N_2(g)$ and for Xe(g). The effusion rate of the doser [$(1.90\pm0.06)\times10^{14}$ torr second for a hypothetical 1 amu molecule] remained constant to within ±3% for four years.

The role of X-radiation in the fluorination of the diamond surface is demonstrated by condensing a thick layer of $C_4F_9I$ on the surface at 119K, irradiating for various times, and then desorbing the remaining $C_4F_9I$ by heating the surface to 300K. This leaves a strongly-bound chemisorbed F layer which yields a F(1s) XP spectrum with a feature at a binding energy of 687.7 eV. The development of the chemisorbed layer with increasing irradiation is shown by FIG. 2. In the absence of X-ray irradiation, no dissociative chemisorption occurs. To avoid the possibility that these effects are due to stray electrons originating from the X-ray source, a control experiment with a bias voltage on the diamond of −200 V is also shown in FIG. 2 (open data point), and no significant effect on the results was observed.

The XPS characteristics of the diamond surface were measured with a Leybold-Heraeas EA-11 spectrometer, using Mg Kα X-ray radiation. Cu Lα impurity X-ray ghost features were also present. The X-ray source operated at 15 kV; 20 mA; 300 W. The spectrometer pass energy was set at $\Delta E=45$ eV, and 30 scans of the desired energy range were obtained (unless noted otherwise). The binding energy scale was calibrated using a sputter-cleaned Au or Cu standard which was positioned at the focal point of the XPS. During experiments, the small Mo(3d) features originating from the clean Mo surface support also verified that the energy scale remained fixed. The maximum binding energy errors were ±0.05 eV. Separate studies indicate that negligible (0.018 eV) surface charging occurs under the measurement conditions employed here. All XPS core level intensities are integrated over the line width, using a linear baseline.

The integrated XPS intensities of the F(1s), I(3d) and diamond C(1s) transitions following exposure of the surface to $5\times10^{16}$ $C_4F_9I/cm^2$ at 119K are shown in FIG. 3. This results in the deposition of a thick condensed layer of $C_4F_9I$. Both $CF_2$ and $CF_3$ groups are detected in the C(1s) spectrum of the thick overlayer. Upon heating to 300K, both the F(1s) and I(3d) intensities decreased significantly as molecular $C_4F_9I$ desorption occurred. The removal of the thick $C_4F_9I$ layer is accompanied by an increase of the diamond-C(1s) intensity as overlayer screening effects are decreased. It is seen in FIG. 3 that both $CF_3$— and $CF_2$—C(1s) features are observed on the diamond (100) surface following photolysis of the overlayer and subsequent removal of unphotolyzed $C_4F_9I$ by desorption at 300K. In addition, both I(3d) and F(1s) features corresponding to chemisorbed species on the diamond surface are visible following photolysis and removal of the remaining $C_4F_9I$ layer by heating.

Temperature programming of the diamond crystal was achieved between about 119K and 1450K using a feedback controller. All heating cycles were carried out at a controlled heating rate of ~3.4K/s, followed by immediate cooling from the maximum temperature reached in each cycle.

Mass spectrometric measurements of desorbing species were carried out using a line-of-sight geometry from the crystal into the differentially pumped mass spectrometer ionizer, through a 2.0 mm diameter aperture mounted on the quadrupole mass spectrometer (QMS) axis. The front of face of the diamond (100) crystal was reproducibly positioned 1 mm from the QMS aperture. Spurious electron bombardment effects on the diamond surface from the QMS thermionic emitter were avoided by using a −100 V bias on the aperture. Temperature programmed desorption (TPD) was monitored with a VTI multiplex controller which involves a cycle of 3 mass peaks (as well as temperature readings) being monitored in a period of ~0.4 s.

LEED experiments were performed using a homebuilt 4 grid (2 hemispherical and 2 flat) detector which utilizes dual microchannel plate amplification prior to a phosphor display screen. A Sharp video camera was used to record the LEED data during data acquisition. A Varian model 981-2145 electron gun with added x and y deflection plates On addition to an external gimble assembly) was used for the LEED studies. The primary energy ($E_p$) of the incident electrons was 135 eV$<E_p<$185 eV, and the current measured at the crystal (vs. ground) was <1 nA.

$C_4F_9I$ (97% min. purity) and $CF_3$ (99.7% min. purity) were obtained from PCR Inc. and were used without further purification, except for freeze-pump-thaw cycles for $C_4F_9I$.

X-radiation was able to dissociate both $C_4F_9I$ and $CF_3I$ when deposited as condensed layers on the diamond surface at about 119K. All measurements were made following a uniform X-ray exposure of about 180 minutes to the fluoroalkyl iodide overlayer. Following thermal desorption of the excess fluoroalkyl iodide, diamond fluorination was observed.

The behavior of the F(1s), I($3d_{5/2}$) and the diamond C(1s) intensities as the diamond (100) surface is heated in ultrahigh vacuum after fluorination by X-ray irradiation of the $C_4F_9I$ overlayer is shown in FIG. 4. Upon heating, the I($3d_{5/2}$) intensity decreases to zero at 400K. Heating to ~650K causes a slow asymptotic decrease in the F(1s) intensity and the diamond C(1s) intensity increased further. Above ~900K, the F(1s) intensity slowly decreased as the diamond surface was heated to 1500K.

The changes which are observed in the C(1s) features corresponding to $CF_2$ and $CF_3$ moieties during heating are shown in FIG. 5. The ratio of the integrated intensities of the two C(1s) features, $CF_2/CF_3=2.8\pm0.1$ for the top spectrum of FIG. 5. For the $C_4F_9$ chemisorbed species, this ratio is 3.0 in

the absence of self-screening effects. This ratio remained approximately constant at ~2.8±0.3 in the temperature range from 300K to 650K as the anchored $C_4F_9$ species gradually decompose. This indicates that anchored $CF_3(CF_2)_3$— species slowly thermally decompose on the surface in the temperature range 300K to ~700K, leaving chemisorbed F.

The F(1s) spectra obtained as a function of heating temperature for the layer produced from $C_4F_9I$ photolysis are shown in FIG. 6. At 300K, two overlapping F(1s) transitions with binding energies of 687.7 eV and ~685.8 eV are observed. Heating from 300K to ~850K caused the yield of the 687.7 eV F(1s) transition to decrease to near zero. Since the $CF_3$— and $CF_2$—C(1s) intensities also decrease to zero in approximately this same temperature range. The F(1s) transition at 687.7 eV is assigned to the fluorine atoms in the $CF_3(CF_2)_3$— surface species chemisorbed on the diamond substrate. The second F(1s) transition at a binding energy of ~685.8 eV is more clearly revealed as the $C_4F_9$ surface species thermally decompose. This second F(1s) feature begins to decrease in intensity at ~850K and continues to do so up to 1500K. The ~685.8 eV F(1s) feature is assigned to chemisorbed F on the diamond (100) surface.

Semiconductor surfaces are often passivated by the chemisorption of surface H which caps the dangling bonds. This effect is investigated by carrying out the photolysis of a $C_4F_9I$ overlayer on D-passivated diamond (100). X-ray irradiation of the layer causes two pairs of spin-orbit split I(3d) states to appear as shown in FIG. 7. The higher binding energy pair of I(3d) states is due to iodine in the undecomposed $C_4F_9I$ molecules held on the surface. The second pair of states (shifted above 5 eV to lower binding energy) is assigned to DI molecules trapped in the $C_4F_9I$ condensed layer at 119K. These results indicate that I atoms released by photolysis of the C—I bond effectively attack surface C—D bonds on the diamond, causing D abstraction at 119K. It is reasonable to expect that the abstraction in these experiments would also occur for surface C—H groups since D and H would behave similarly. Chemical bonding of F to surface sites on the diamond (100) occurs on heating the surface, indicating that hydrogen passivation is ineffective for photochemical fluorination.

Because of the complexity of the $C_4F_9I$ molecule, detailed studies of the photoactivation of $CF_3I$ on diamond (100) have also been carried out. The clean crystal is exposed to $CF_3I(g)$ at a diamond surface temperature of 119K. Adsorption is observed, causing attenuation of the diamond C(1s) feature. FIG. 8 shows the F(1s), C(1s), I(3d), regions of the XP spectra following exposure $5\times10^{16}$ $CF_3I/cm^2$ at 119K. In addition to these measurements at high $CF_3I$ exposure, both the F(1s) and the I(3d) XPS features are observed from the overlayer following an exposure of $2.5\times10^{14}$ $CF_3I/cm^2$ (data not shown). FIG. 9 shows a plot of the integrated diamond C(1s) [circles], F(1s) [triangles], and $I(3d_{5/2})$ [squares] peak areas as a function of $CF_3I$ exposure at a diamond (100) temperature of 119K. The open data points represent adsorption experiments performed using D#2, and filled data points represent adsorption experiments performed using D#1. The data on the two diamonds are normalized using the diamond C(1s) intensity (following heating to 1450 K) as a method to judge small differences in X-ray intensity and crystal geometry. It is seen for $CF_3I$ that the rate of adsorption at 119K decreases significantly above an exposure of ~$1\times10^{16}$ $CF_3I/cm^2$.

An important observation is that on heating the $CF_3I$-treated surface the diamond-related C(1s) feature does not shift to higher binding energy until the adsorbed layer is heated to ~250K. This binding energy increase is indicative

that the photochemical fragments from $CF_3I$ form strong chemisorption bonds with the diamond surface only after the overlayer has been heated to induce mobility of the photofragments.

FIG. 10 shows, schematically, for an n-doped diamond crystal, upward band bending in the presence of partially filled surface states. F adsorption will produce a positive shift in the C(1s) peak bonding energy relative to the Fermi energy for the carbon atoms detected in the surface and subsurface region of the diamond as the bands flatten.

The observed photoprocesses for both $C_4F_9I$ and $CF_3I$ are likely due to a variety of processes induced by the X-radiation incident on the condensed layers of these molecules. Certainly direct excitation by X-rays, leading to photoionization processes causes dissociation of the molecules. In addition, secondary electron emission from the irradiated substrate is effective in breaking the C—I bonds in the fluoroalkyl iodide molecules. In FIG. 2 it is shown that the production of chemisorbed F atoms on the diamond surface is directly dependent on the time of irradiation of the condensed overlayer of $C_4F_9I$. It is well known that the weak C—I bond are photochemically broken in the alkyl iodides. FIG. 4 displays the thermal stability pattern of the surface fluorine species.

FIGS. 3 and 5 clearly indicate that $C_4F_9$ groups are able to be adsorbed on diamond (100) following photodissociation of $C_4F_9I$ overlayers. The presence of $CF_2$ and $CF_3$ moieties in an approximate 3 to 1 ratio is found over the temperature range of their stability extending up to about 750K as judged from the two C(1s) features in FIG. 5. The detection of these moieties is indicative of chemisorbed $C_4F_9$ groups on the diamond surface. Studies in FIG. 6 of the F(1s) states at binding energies of 687.7 eV and ~685.8 eV correlate fairly well with the thermal behavior of the $CF_2$ and $CF_3$ groups in FIG. 5. The lower binding energy F(1s) state is assigned to chemisorbed F on diamond (100), produced from the thermal decomposition of the $C_4F_9$ groups below about 900K.

It is clear from FIG. 7 that photodissociation of the C—I bonds in $C_4F_9I$ overlayers at 119K leads to hydrogen abstraction from the hydrogen-passivated diamond, producing trapped hydrogen iodide species. This is a very fortunate situation, enhancing the use of fluoroalkyl iodides for photochemical fluorination of diamond under practical conditions, since natural diamond surfaces are generally passivated by a hydrogen overlayer and might be expected to be unreactive. Thus, photochemistry of the fluoroalkyl iodides not only supplies active fluoroalkyl groups for attachment to the diamond, but also supplies iodine atoms for extraction of the surface hydrogen species making surface sites available for fluoroalkyl surface bonding.

At 119K, $CF_3I$ adsorbs molecularly onto diamond (100). Upon heating to about 140K, molecular $CF_3I$ desorption is detected by mass spectrometry. In this same temperature range, both the F(1s) and I(3d) signals decrease in yield while the C(1s) yield from the diamond substrate increases.

The use of $C_4F_9I$ as a fluorinating agent produces higher coverages of chemisorbed F than may be achieved using comparable conditions with $CF_3I$ overlayers. For $C_4F_9I$, the value of $N_F/N_C$ at 300K is 2.0 on diamond #1; upon heating to 700K, $N_F/N_C$=0.6, where $N_F/N_C$ is the ratio of fluorine atoms to surface carbon atoms. For $CF_3I$-produced layers at 300K, $N_F/N_C$=0.10–0.17.

At diamond (100) surface temperatures near 300K, all $CF_3$ species (from $CF_3I$) have dissociated. For $C_4F_9$ species, all $CF_3(CF_2)_3$ groups have dissociated by about

9

750K–900K. At higher temperatures, depletion of surface fluorine begins to occur by a desorption process. This process occurs over a very wide temperature range culminating at ~1500K. The final F-depletion process appears to be similar for the two fluorinated iodides. For an n-doped diamond crystal (upward band bending in the presence of partially filled surface states), F adsorption will produce a positive shift in the C(1s) peak binding energy relative to the Fermi energy for the carbon atoms detected in the surface and subsurface region of the diamond as the bands flatten, as shown schematically in FIG. 10. Similar shifts were noted when the diamond (100) surface was exposed to atomic D. For atomic D, the C(1s) binding energy shift, at saturation, was ~+0.9 eV (for D#2). Upon fluorination, the C(1s) binding energy shift was ~+0.4 eV (for D#2) and was less than ~+0.1 eV for D#1. This comparison between D and F induced shifts is easily rationalized considering that the F coverage is less than 1 ML, whereas very high exposures to atomic D were employed.

An improved method for the fluorination of diamond surfaces using radiation-induced or ultraviolet light-induced activation of perfluoroalkyl iodide molecules adsorbed on the diamond surface is disclosed. The anchored fluoroalkyl groups provide an easily controlled source of fluorine for the production of chemisorbed fluorine on the diamond surface. The chemisorbed fluorine thermally decomposes over a temperature range from about 700K to 1500K. The fluorinated diamond surface has thermal stability to 1500K. The presence of passivating surface C—H groups on the diamond does not inhibit fluorination by this method. A fluorinated diamond product is made by this method.

Where particular embodiments of the present invention have been described above, for purposes of the illustration, it will be evident to those skilled in the art that numerous variations of the details may be made without departing from the invention as defined in the appended claims.

What is claimed is:

1. A method for the fluorination of a diamond surface comprising:

10

depositing a layer of perfluorinated alkyl iodides having the formula $C_nF_{2n+1}I$ on said diamond surface wherein n is a positive integer from 1 to 13;

producing perfluorinated alkyl free radicals by photodecomposing C—I bonds of said perfluorinated alkyl iodides on said diamond surface;

forming a perfluorinated alkyl layer by anchoring said photochemically induced perfluorinated alkyl free radicals to said diamond surface; and

decomposing said perfluorinated alkyl layer on said diamond surface to produce chemisorbed fluorine on said diamond surface.

2. The method of claim 1, employing as said perfluorinated alkyl iodide $C_nF_{2n+1}I$ selected from the group consisting of wherein n=1 to 5 to cause fluorination of said diamond surface.

3. The method of claim 2, including establishing by said process greater than one fluorine atom per surface carbon atom chemisorbed on said diamond surface.

4. The method of claim 3, wherein n=4 including effecting retention of chemisorbed fluorine to remain on said diamond surface from about 500 to 1500K.

5. The method of claim 4, including effecting photodecomposition of said perfluoroalkyl iodide on said diamond surface by at least one of X-radiation or ultraviolet light.

6. The method of claim 5, including employing a temperature of about 120 to 300K to desorb excess perfluoroalkyl iodide on said diamond surface.

7. The method of claim 6, including employing a temperature of about 300K to 700K to decompose said perfluorinated alkyl layer to produce said chemisorbed fluorine on said diamond surface.

8. The method of claim 7, including employing iodine atoms from said perfluoroalkyl iodides to extract hydrogen from said diamond surface.

* * * * *